EUROPEAN JOURNAL OF PURE AND APPLIED MATHEMATICS
2025, Vol. 18, Issue 4, Article Number 7147
ISSN 1307-5543 – ejpam.com
Published by New York Business Global

Complex Neutrosophic Soft Topology with Multivariate Analysis: A Unified Framework for Signal-Template Relationships

Maha Mohammed Saeed[1], Raed Hatamleh[2], Hamza Ali Abujabal[3], Aqeedat Hussain[4], Arif Mehmood[4], M. I. Elashiry[5], Abdelhalim Hasnaoui[5], Alaa M. Abd El-latif[5,*]

[1] *Department of Mathematics, Faculty of Sciences, King Abdulaziz University, P.O. Box 80203, Jeddah 21589, Saudi Arabia*
[2] *Department of Mathematics, Faculty of Science, Jadara University, P.O. Box 733, Irbid 21110, Jordan*
[3] *Department of Mathematics, King Abdulaziz University, P.O. Box 80003, Jeddah 21589, Saudi Arabia*
[4] *Department of Mathematics, Institute of Numerical Sciences, Gomal University, Dera Ismail Khan 29050, KPK, Pakistan*
[5] *Department of Mathematics, College of Science, Northern Border University, Arar 91431, Saudi Arabia*

Abstract. A novel theoretical method based on the topological formulation of complex neutrosophic soft sets (CNSS) is presented in this work. We go on to provide a thorough one-value complex neutrosophic soft topology, defining the most important topological properties such as interior, closure, and other related theoretical concerns, in order to give a strong mathematical foundation. An example is then provided to illustrate this framework's analytical capabilities. To ensure a thorough empirical validation of this paradigm, we employ a multifaceted approach that combines PCA, clustering, and manifold learning. Everyone agreed that a clear target hierarchy should be established, even though we employed a variety of analytical methodologies. In this hierarchy, T_1 was consistently described as the most stable and representative target, T_2 as a transitional outlier, and T_3 as the most divergent target. In its most basic form, multivariate analysis and topological theory offer a versatile framework for clarifying the connections between templates and signals while avoiding the drawbacks of over-methodologization.

2020 Mathematics Subject Classifications: 03E72, 06F25, 62H25, 54A10

Key Words and Phrases: Complex neutrosophic soft sets, complex neutrosophic soft topology, cotangent similarity measures, data visualization techniques

1. Introduction

Garg and Rani studied the aggregation operators of Complex Interval-Valued Intuitionistic Fuzzy Sets [2], whereas Al-Qudah and Hassan studied the functions of Complex Multi-Fuzzy Sets [1]. In the event that there are several possible complex evaluations, Garg et al. later presented Complex Hesitant Fuzzy Sets, which include additional distance measures [3]. Singh constructed a concept lattice using Complex Vague Sets to illustrate the versatility of these

*Corresponding author.
DOI: https://doi.org/10.29020/nybg.ejpam.v18i4.7147

Email addresses: mmmohammed@kau.edu.sa (M. M. Saeed), raed@jadara.edu.jo (R. Hatamleh), haabujabal@kau.edu.sa (H. A. Abujabal), aqeedathussain04@gmail.com (A. Hussain), mehdaniyal@gmail.com (A. Mehmood), mustafa.elashiry@nbu.edu.sa (M. I. Elashiry), abdllhalim.hasanawa@nbu.edu.sa (A. Hasnaoui), alaa.ali@nbu.edu.sa (A. M. Abd El-latif)

ideas [4]. Scientists have expanded their conceptual richness and applicability based on the basic frameworks of complicated neutrosophic sets. Its ability to capture both the positive and negative memberships of truth and indeterminacy and falsity in the complex plane makes it a significant extension, first presented by RaBroumi et al. as Bipolar Complex Neutrosophic Sets [5]. As a result, it is a more effective tool for use in decision-making problems where opposing factors are present.

Al-Quran and Alkhazaleh studied the significance of the relations between complicated neutrosophic sets [7], and Quek et al. [6] constructed the sets in the theoretical framework of graph theory. Linguistic solutions to interval complicated neutrosophic sets were provided by Dat et al. [8] to bridge the gap between the numerical and linguistic representations, making them more useful in human-based decision-making scenarios. Molodtsov introduced Soft Set Theory, another similarly potent paradigm for handling uncertainty, at the same time [9].

This gave a totally new, parameterized manner of treating imprecision that was not subject to the limits of the old-fashioned membership functions. The combination of pre-existing fuzzy models and soft sets quickly became a productive area of study. Maji et al. made the initial attempt at this synergy when they launched fuzzy soft sets [10] and intuitionistic fuzzy soft sets [11], which parameterized soft sets but with fuzzy and intuitionistic fuzzy set capability, respectively. This trend of hybridization continued to embrace increasingly intricate forms of uncertainty. The researchers that had to deal with uncertain membership information developed Interval-Valued Fuzzy Soft Sets [12] and Interval-Valued Intuitionistic Fuzzy Soft Sets [13]. Moreover, neutrosophic theory was adopted with the introduction of Neutrosophic Soft Sets by Maji [14] and Interval-Valued Neutrosophic Soft Sets by Deli [17]. These two unconnected concepts describe the truth, indeterminacy, and falsity of parameters separately.

Abu Qamar and Hassan's [18] introduction of the Q-Neutrosophic Soft Set, which demonstrates the contemporary and dynamic intersection of complex, neutrosophic, and soft set theories to handle the complexity of uncertainty in data, is one of the even more extended forms of the area that are now being explored. More sophisticated and specialized models have been produced as a result of the ongoing hybridization trend. By studying the algebraic structures of Q-neutrosophic soft fields, Abu Qamar et al. developed the theoretical foundation of the study and further formalized the work on Q-Neutrosophic Soft Sets [19].The model's ability to progress from pure set theory to standard algebraic frameworks was a sign of its maturity. The actual merger of soft set theory and the multifaceted fuzzy model was another noteworthy parallel comparable development. It resulted in the Complex Fuzzy Soft Set [20], a paradigm that leverages the two-dimensional information store of complex membership degrees and the parameterization of soft sets. Soon after, this hybrid was expanded to handle greater imprecision, giving rise to the Interval-Valued Complex Fuzzy Soft Set [21]. Recent advances have proposed even more powerful hybrid frameworks that can simulate complicated and higher-order uncertainty, pushing this integration to even greater heights. As an example, Fujita [22] developed strong models that can handle data represented by multi-dimensional membership degree by incorporating a hyper-fuzzy environment into the already outstanding VIKOR and DEMATEL approaches. In the same vein, Gul [23] proposed a bipolar fuzzy rough set model fused with the VIKOR approach, which offers a more detailed model on the capacity to manage conflicting criteria and is useful in reflecting the positive and negative preferences of decision-makers in a d-covering context. Alongside these advancements, the study of more complex algebraic structures has produced a solid theoretical foundation for the use of these methods in significant fields. The work of Abdalla et al. [24] on Interval-Valued Fermatean Neutrosophic Super Hyper Soft Sets is an illustration of this trend. It describes how complex forms of uncertainty in real-world contexts like health care, where the information is indeterminate, incomplete, and may come from multiple sources, can be represented by sophisticated set-theoretic models.

1.1. Literature Review

The recent study by AlAkram et al. [25], which suggested Complex Fermatean Fuzzy N-Soft Sets, is one example of how novel this is at the moment. This model is a significant amalgam of many potent paradigms: These three cutting-edge ideas are combined in this hybrid model to provide an unparalleled capacity for handling multi-level, complicated, and ambiguous data while making decisions. Its creation demonstrates the field's constant drive to create increasingly expressive and adaptable mathematical tools in order to represent the complexity of the real world. By establishing the Complex Bipolar-Valued Neutrosophic Soft Set [26], Al-Quran et al. advanced the research of bipolarity on the complex neutrosophic framework and improved the model's ability to handle contradictory data dimensions. Akram et al. produced Complex Neutrosophic N-Soft Sets [27], which provide a multi-level graded structure of truth, indeterminacy, and falsity, by combining the influential idea of N-soft sets with neutrosophic theory in complex space. Formally describing the complex neutrosophic soft expert relation [28], which provides a mathematical foundation for comparing and connecting the many expert evaluations in this intricate framework, was a significant theoretical and practical leap. A theory of Interval-Valued Complex Neutrosophic Soft Sets [29] and related relations [31] also extended this relational paradigm to address imprecision. When these models were eventually articulated in complex space [30], it was a necessary generalization, and their representational power was significantly increased. Effective comparison tools are essential to all of these advancements. Similarity measurements, which are essential for applications like pattern recognition and medical diagnosis, have been the subject of extensive research as a result. Numerous structures have been developed, including Lattice Ordered Multi-Fuzzy Soft Sets [33], Single and Multi-Valued Neutrosophic Hypersoft Sets [32], and m-polar-interval valued Neutrosophic Soft Sets [34]. The real-world effects of such progressively abstract theoretical constructions are demonstrated by the practical effects of such measurements, particularly in sensitive fields like medical diagnostics [34], which completes the circle between the formulation of mathematical issues and their practical resolution. Since the proliferation of these sophisticated hybrid forms has necessitated the development of robust methods for comparing and contrasting these forms, recent studies have included research on similarity metrics and entropy. They are crucial in applications like as pattern recognition, medical diagnosis, and multi-criteria decision-making, where the ability to measure the degree of similarity or ambiguity across different sets is crucial. Basic similarity measures between neutrosophic and interval neutrosophic sets were founded by Broumi and Smarandache [38] and Ye [39], respectively. These were soon generalized to hybrid structures, as was the case with similarity measures of Interval Valued Neutrosophic Soft Sets [40]. Medical usages are also a dominant factor and Liu et al. [35] utilize the Euclidean distance to neutrosophic sets to diagnose, which Zulqarnain et al.[34] apply to more advanced m-Polar features. The comparison techniques grew more intricate as the models became more intricate. The researchers employed Lattice Ordered Multi-Fuzzy Soft Sets [33], Possibility Intuitionistic Fuzzy Hyper-soft Sets [37], and T-Spherical Fuzzy Sets [36] as special measures. The same idea holds true in the complex realm, where Complex Multi-Fuzzy Soft Sets [42] have been subjected to entropy and similarity measures in order to handle the dimensional expansion. Additionally, equivalent entropy and distance metrics have been added to generalization to structures like Q-Neutrosophic Soft Sets [41], ensuring that even the most generalized models have the mathematical resources needed to be practical. To put it simply, the creation of each new hybrid model is now entangled with the creation of the corresponding entropy and similarity metrics. This ensures that the theoretical power of such complex structures can be appropriately applied to the solution of complex real-world problems where comparison and uncertainty quantification are the best qualities. In order to address the issue of multi-criteria group decision-making, Xu et al. focused on distance measures of Interval Complex Neutrosophic Sets [44], while Selvachandran et al. developed a similarity measure on Complex Vague Soft Sets and demonstrated its applicability in pattern recognition [43]. These metrics of comparison have been developed and

applied extensively on a variety of complex hybrid models. Neutrosophic set and its characteristics were studied in [45].

A fundamental idea in the field is brought to light by this consistent correlation between the new set-theoretic models and specially designed similarity and distance measures: the practice drives and validates the theory's progress. Lastly, our ability to mathematically describe uncertainty has grown exponentially since the original fuzzy sets proposed by Zadeh [46] evolved into the complex, neutrosophic, and soft hybrid models of today. This has been called a cycle of innovation, whereby a new theoretical framework is created by identifying a representational deficiency, then new components are added, and finally, real-world applications of similarity measures and aggregation operators are added to deal with the real world. The result is a multifaceted and varied ecosystem of mathematical tools that can simulate the gradation, ambiguity, cyclicality, and intrinsic contradictions of complex systems, enabling robots to reason more like humans. Since the principles of these frameworks have been extended beyond set theory to abstract algebraic and mathematical structures, the final step of the evolutionary process demonstrates how theoretically profound they are. This development was supported by the introduction of Interval Neutrosophic Sets [48] and is based on Smarandache's early work on Neutrosophy [47], which provides the logical and philosophical underpinnings of neutrosophic logic. Fuzzy, intuitionistic, and neutrosophic notions can now be applied to basic algebraic fields thanks to this groundbreaking discovery. The operations of Intuitionistic and Interval-Valued Intuitionistic Fuzzy Soft Sets [49] have been more extensively generalized to distance measurements, which gives them an algebraic basis. Concurrently, the set-theoretic models have been expanded to include more complex models that can process multi-dimensional attribute values, as the Plithagenic Hyper-soft Set [50].

Most significantly, a robust research thread that builds algebraic systems on top of the existing uncertainty-based foundations has been produced. These include studies of structures like Intuitionistic Anti Fuzzy Normal Subrings over Normed Rings [52] and the Neutrosophic Multiplication Module [51]. The work on Polish Groups [53], conditions on P. P. Rings [54], Classical Artinian Modules [55], Fractional Ideals [56], and structures in Topological Groups [57] all point to a parallel study program in pure algebra that is extended by this subject.

This indicates that in addition to advancing these uncertainty theories, the mathematical community is also contributing to the advancement of the classical algebraic structures to which they are applied. In conclusion, it is important to note that the current state of amazing intellectual synergy is a direct result of the fuzzy sets of Zadeh. Beginning with the very simple idea of graded membership, it evolved into a whole ecosystem of models to address uncertainty through phases of integration and generalization to complex planes, neutrosophic logic, and parameterized soft sets. This evolution typically follows a positive feedback loop: theoretical innovation results in new hybrid models, which are then given useful tools like comparable measures to be applied, and their ideas are abstracted to enhance fundamental fields like abstract algebra. This leads to a dynamic and intricate area of mathematics that ultimately enhances our ability to reason, model, and navigate a world that is fundamentally complex and uncertain. The thorough examination of the structures, like the Neutrosophic Multiplication Module [51] and Intuitionistic Anti Fuzzy Normal Sub-rings over Normed Rings [52], continues this robust line of inquiry that seeks to create algebraic systems with uncertainty-driven foundations. As evidenced by work on Classical Artinian Modules [58], Polish Groups [53], conditions on P.P. Rings [54], Fractional Ideals [56], and the study of new types of mappings in Topological spaces with Strongly Closed Graphs [59], this line of inquiry is part of a larger, parallel research program in pure algebra and topology.

The investigation of supra open soft sets and its various decompositions and applications, as well as soft set theory, are both superseded by supra soft topology, according to the sources provided. Fundamental results on decompositions of supra soft sets, together with the concept of soft continuity in this context, were provided by El-Sheikh and Abd Ellatif's basic contribu-

tions [60]. Supra soft strongly generalized closed sets [62], supra soft strongly extra generalized closed sets [63], and supra soft strongly *semi*∗ generalized closed sets [65] are only a few of the specific classes of soft sets that are now being studied in this field. Furthermore, the ideas have been crucial in defining and researching different forms of soft connectedness [67] as well as related soft separation axioms [61][64][66]. The research of supra soft compactness [69] and interactions with soft ideals [68] have also contributed to the development of the theory.
The creation of complicated frameworks that can manage uncertainty, indeterminacy, and intricate relationship systems has greatly influenced recent developments in computational mathematics and logic. Among these, neutrosophic theory has shown itself to be an effective tool for simulating real-world issues. It generalizes fuzzy and intuitionistic fuzzy sets by adding a truth-membership, indeterminacy-membership, and falsity-membership function. Its wide range of uses, from resolving complicated differential equations [70] to examining structural characteristics in algebra and graph theory [71, 72], demonstrate this. Simultaneously, research into hybrid systems that combine fuzzy and neutrosophic sets with other mathematical fields continues to provide new discoveries. For example, recent research has established complex tangent trigonometric methods for advanced fuzzy sets [73] and extended complex cubic intuitionistic fuzzy sets to algebraic structures [74]. Additionally, the analysis of minimal units in fuzzy neutrosophic rings [76] and the foundational work on topological spaces using symbolic n-plithogenic intervals [75] show the growing frontier of this field, offering a solid mathematical foundation for addressing problems with inherent ambiguity and multifaceted information.

1.2. Novelty and Motivation for Research

For the first time, a one-value complex neutrosophic soft topology that strictly satisfies the fundamental features, notably the closure and the interior, is developed by combining the topological formulation with complex neutrosophic soft sets (CNSS). Such a study formalizes a topological basis that ensures theoretical coherence and generalizability, in contrast to the present neutrosophic or soft set methodologies, which are mostly algebraic or descriptive.
The relationship between this abstract model and specific analytical methods, such as PCA, clustering, and manifold learning, is truly novel since it demonstrates how an entirely mathematical model can be applied directly to empirical classification and pattern recognition issues. Although it does not rely too much on any one approach, this interdisciplinary connection between theory topology and real-world multivariate analysis ensures interpretability and strength. The limitations of the existing classification and similarity metrics to address ambiguity, instability, and divergence in signal-template connections have been the driving force behind this investigation. When dealing with intermediate instances, such as T_2, that do not fully fall into either the stability or the divergence category, conventional procedures are extremely challenging. This study aims to propose a topological framework that implements neutrosophic uncertainty handling in a way that is both theoretically rigorous and practically adaptive, generating consistent target hierarchies. One solid argument for the need for such a unified paradigm is the consensus that T_1 is the most stable, T_2 is intermediate and transitional, and T_3 is divergent in different analytical lenses. The ultimate objective of the study, however, is to balance the practicality of the empirical data with the depth of concepts in order to ensure that complicated signal systems may be accurately and vividly interpreted while being open to analysis.

2. Preliminaries

In this section, we will give some preliminary information for the present study.

Definition 1. *[45] A neutrosophic set A on the universe of discourse X is defined as:*

$$A = \{\langle x, T_A(x), I_A(x), F_A(x)\rangle : x \in X\}$$

where, $T, IF : X \longrightarrow]0,1[$ and $0 \leq T_A(x) + I_A(x) + F_A(x) \leq 3$.

Definition 2. *[9] Let X be an initial universe, E be a set of all parameters and $P(X)$ denotes the powerset of X. A pair of (F, E) is called a soft set over X, where F is a mapping given by $F : E \longrightarrow P(X)$. In other words, the soft set is a parameterized family of subsets of the set$X$. For $e \in E, F(e)$ may be considered as the set of e-elements of the soft set (F, E), or as the set of e-approximate elements of the soft set, i.e.,*

$$(F, E) = \{(e, F(e)) : e \in E, F : E \longrightarrow P(X)\}$$

Firstly, neutrosophic soft set defined by Maji [14] and later this concept has been modified by Deli and Broumi [15] as given below:

Definition 3. *Let X be an initial universe, E be a set of all parameters. Let $P(X)$ denote the set of all neutrosophic sets of X. Then, a neutrosophic soft set $(\tilde{F}.E)$ over X is a set defined by a set valued function $\tilde{F}$ representing a mapping $\tilde{F} : E \longrightarrow P(X)$ where $\tilde{F}$ is called approximate function of neutrosophic soft set $(\tilde{F}, E)$. In other words, the neutrosophic soft set is a parametrized family of some elements of the set $P(X)$ and therefore it can be written as a set of order pairs,*

$$(\tilde{F}, E) = \{(e, \langle x, T_{\tilde{F}(e)}(x), I_{\tilde{F}(e)}(x), F_{\tilde{F}(e)}(x)\rangle : x \in X) : e \in E\}$$

where $T_{\tilde{F}(e)}(x), T_{\tilde{F}(e)}(x), F_{\tilde{F}(e)}(x) \in [0, 1]$, respectively called the truth-membership, indeterminacy-membership, falsity-membership of $\tilde{F}(e)$. Since supremum of each $T, I, Fis1$ so the inequality $0 \leq T_{\tilde{F}(e)}(x) + I_{\tilde{F}(e)}(x) + F_{\tilde{F}(e)}(x) \leq 3$ is obvious.

Definition 4. *[16] Let $(\tilde{F}, E)$ be a neutrosophic soft sets over the universe set X. The complement of $(\tilde{F}, E)$ is denoted by $(\tilde{F}, E)^c$ and is defined by:*

$$(\tilde{F}, E)^c = \{(e, \langle x, F_{\tilde{F}(e)}(x), 1 - I_{\tilde{F}(e)}(x), T_{\tilde{F}(e)}(x)\rangle : x \in X) : e \in E\}$$

Obvious that, $((\tilde{F}, E)^c)^c = (\tilde{F}, E)$.

Definition 5. *[14] Let $(\tilde{F}, E)$ and $(\tilde{G}, E)$ be two neutrosophic soft sets over the universe set X. $(\tilde{F}, E)$ is said to be neutrosophic soft subset of $(\tilde{G}, E)$ if $T_{\tilde{F}(e)}(x) \leq T_{\tilde{G}(e)}(x), I_{\tilde{F}(e)}(x) \leq I_{\tilde{G}(e)}(x), F_{\tilde{F}(e)}(x) \geq F_{\tilde{G}(e)}(x)$, for all $e \in E$, for all $x \in X$. It is denoted by $(\tilde{F}, E) \subseteq (\tilde{G}, E)$. $(\tilde{F}, E)$ is said to be neutrosophic soft set equal to $(\tilde{G}, E)$ if $(\tilde{F}, E)$ is neutrosophic soft subset of $(\tilde{G}, E)$ and $(\tilde{G}, E)$ is neutrosophic soft subset of $(\tilde{F}, E)$. It is denoted by $(\tilde{F}, E) = (\tilde{G}, E)$.*

3. Operations on Complex Single-Valued Neutrosophic Soft Sets

In this section , the operations of union, intersection, difference, AND and OR on complex single-valued neutrosophic soft sets are defined. In addition to this, examples are given for better understanding these operations.

Definition 6. *Let $(\tilde{F}_1, E)$ and $(\tilde{F}_2, E)$ be two complex single-valued neutrosophic soft sets over the universe set X. Then their union is represented by $(\tilde{F}_1, E) \cup (\tilde{F}_2, E) = (\tilde{F}_3, E)$ is defined by:*

$$(\tilde{F}_3, E) = \left\{\left(e, \langle x, T_{\tilde{F}_3(e)}(x), I_{\tilde{F}_3(e)}(x), F_{\tilde{F}_3(e)}(x)\rangle : x \in X\right) : e \in E\right\},$$

Where

$$T_{\tilde{F}_3(e)}(x) = \max\{T_{\tilde{F}_1(e)}(x), T_{\tilde{F}_2(e)}(x)\}$$
$$I_{\tilde{F}_3(e)}(x) = \max\{I_{\tilde{F}_1(e)}(x), I_{\tilde{F}_2(e)}(x)\}$$
$$F_{\tilde{F}_3(e)}(x) = \min\{F_{\tilde{F}_1(e)}(x), F_{\tilde{F}_2(e)}(x)\}$$

Definition 7. *Let $(\tilde{F}_1, E)$ and $(\tilde{F}_2, E)$ be two complex single-valued neutrosophic soft sets over the universe set X. Then their intersection is represented by $(\tilde{F}_1, E) \cap (\tilde{F}_2, E) = (\tilde{F}_3, E)$ is defined by:*

$$(\tilde{F}_3, E) = \left\{ \left(e, \langle x, T_{\tilde{F}_3(e)}(x), I_{\tilde{F}_3(e)}(x), F_{\tilde{F}_3(e)}(x) \rangle : x \in X \right) : e \in E \right\},$$

Where

$$T_{\tilde{F}_3(e)}(x) = \min\{T_{\tilde{F}_1(e)}(x), T_{\tilde{F}_2(e)}(x)\}$$
$$I_{\tilde{F}_3(e)}(x) = \min\{I_{\tilde{F}_1(e)}(x), I_{\tilde{F}_2(e)}(x)\}$$
$$F_{\tilde{F}_3(e)}(x) = \max\{F_{\tilde{F}_1(e)}(x), F_{\tilde{F}_2(e)}(x)\}$$

Definition 8. *Let $(\tilde{F}_1, E)$ and $(\tilde{F}_2, E)$ be two complex single-valued neutrosophic soft sets over the universe set x. Then, $(\tilde{F}_1, E)$ difference $(\tilde{F}_2, E)$ operation on them is denoted by $(\tilde{F}_1, E) \setminus (\tilde{F}_2, E) = (\tilde{F}_3, E)$ and is defined by $(\tilde{F}_3, E) = (\tilde{F}_1, E) \cap (\tilde{F}_2, E)^c$ as follows:*

$$(\tilde{F}_3, E) = \left\{ \left(e, \langle x, T_{\tilde{F}_3(e)}(x), I_{\tilde{F}_3(e)}(x), F_{\tilde{F}_3(e)}(x) \rangle : x \in X \right) : e \in E \right\},$$

where

$$T_{\tilde{F}_3(e)}(x) = \min\{T_{\tilde{F}_1(e)}(x), F_{\tilde{F}_2(e)}(x)\}$$
$$I_{\tilde{F}_3(e)}(x) = \min\{I_{\tilde{F}_1(e)}(x), 1 - I_{\tilde{F}_2(e)}(x)\}$$
$$F_{\tilde{F}_3(e)}(x) = \max\{F_{\tilde{F}_1(e)}(x), T_{\tilde{F}_2(e)}(x)\}$$

Definition 9. *Let $\{(\tilde{F}_i, E) : i \in I\}$ be a family of complex single-valued neutrosophic soft sets over the universe set X. Then,*

$$\bigcup_{i \in I} (\tilde{F}_i, E) = \left\{ \left(e, \langle x, \sup_{i \in I} T_{\tilde{F}_{i(e)}}(x), \sup_{i \in I} I_{\tilde{F}_{i(e)}}(x), \inf_{i \in I} F_{\tilde{F}_{i(e)}}(x) \rangle : x \in X \right) : e \in E \right\}.$$

$$\bigcap_{i \in I} (\tilde{F}_i, E) = \left\{ \left(e, \langle x, \inf_{i \in I} T_{\tilde{F}_{i(e)}}(x), \inf_{i \in I} I_{\tilde{F}_{i(e)}}(x), \sup_{i \in I} F_{\tilde{F}_{i(e)}}() \rangle : x \in X \right) : e \in E \right\}.$$

Definition 10. *Let $(\tilde{F}_1, E)$ and $(\tilde{F}_2, E)$ be two complex single-valued neutrosophic soft sets over the universe set X. Then, the AND operation on them is denoted by $(\tilde{F}_1, E) \wedge (\tilde{F}_2, E) = (\tilde{F}_3, E \times E)$ and is defined by:*

$$(\tilde{F}, E \times E) = \left\{ \left((e_1, e_2), \langle x, T_{\tilde{F}_3(e_1,e_2)}(x), I_{\tilde{F}_3(e_1,e_2)}(x), F_{\tilde{F}_3(e_1,e_2)}(x) \rangle : x \in X \right) : (e_1, e_2) \in E \times E \right\}.$$

where

$$T_{\tilde{F}_3(e_1,e_2)}(x) = \min\left\{ T_{\tilde{F}_1(e_1,e_2)}(x), T_{\tilde{F}_2(e_1,e_2)}(x) \right\},$$
$$I_{\tilde{F}_3(e_1,e_2)}(x) = \min\left\{ I_{\tilde{F}_1(e_1,e_2)}(x), I_{\tilde{F}_2(e_1,e_2)}(x) \right\},$$
$$F_{\tilde{F}_3(e_1,e_2)}(x) = \max\left\{ F_{\tilde{F}_1(e_1,e_2)}(x), F_{\tilde{F}_2(e_1,e_2)}(x) \right\}.$$

Definition 11. *Let $(\tilde{F}_1, E)$ and $(\tilde{F}_2, E)$ be two complex single-valued neutrosophic soft sets over the universe set X. Then, the OR operation on them is denoted by $(\tilde{F}_1, E) \vee (\tilde{F}_2, E) = (\tilde{F}_3, E \times E)$ and is defined by:*

$$(\tilde{F}, E\times E) = \left\{\left((e_1,e_2), \langle x, T_{\tilde{F}_3(e_1,e_2)}(x), I_{\tilde{F}_3(e_1,e_2)}(x), F_{\tilde{F}_3(e_1,e_2)}(x)\rangle : x \in X\right) : (e_1,e_2) \in E\times E\right\}.$$

where

$$\begin{aligned} T_{\tilde{F}_3(e_1,e_2)}(x) &= \max\left\{T_{\tilde{F}_1(e_1,e_2)}(x), T_{\tilde{F}_2(e_1,e_2)}(x)\right\}, \\ I_{\tilde{F}_3(e_1,e_2)}(x) &= \max\left\{I_{\tilde{F}_1(e_1,e_2)}(x), I_{\tilde{F}_2(e_1,e_2)}(x)\right\}, \\ F_{\tilde{F}_3(e_1,e_2)}(x) &= \min\left\{F_{\tilde{F}_1(e_1,e_2)}(x), F_{\tilde{F}_2(e_1,e_2)}(x)\right\}. \end{aligned}$$

Definition 12. *A complex single-valued neutrosophic soft set $(\tilde{F}, E)$ over the universe set X is said to be a null complex single-valued neutrosophic soft set if*

$$T_{\tilde{F}(e)}(x) = 0, \quad I_{\tilde{F}(e)}(x) = 0, \quad F_{\tilde{F}(e)}(x) = 1, \quad \forall\ e \in E, \forall\ x \in X.$$

It is denoted by $0_{(X,E)}$.

Definition 13. *A complex single-valued neutrosophic soft set $(\tilde{F}, E)$ over the universe set X is said to be a absolute complex single-valued neutrosophic soft set if*

$$T_{\tilde{F}(e)}(x) = 1, \quad I_{\tilde{F}(e)}(x) = 1, \quad F_{\tilde{F}(e)}(x) = 0, \quad \forall\ e \in E, \forall\ x \in X,$$

Clearly,

$$0^c_{(X,E)} = 1_{(X,E)}, \quad 1^c_{(X,E)} = 0_{(X,E)}.$$

Proposition 1. *Let $(\tilde{F}_1, E)$, $(\tilde{F}_2, E)$ and $(\tilde{F}_2, E)$ be three complex single-valued neutrosophic soft sets over the universe set X. Then,*

(i) $(\tilde{F}_1, E) \cup [(\tilde{F}_2, E) \cup (\tilde{F}_3, E)] = [(\tilde{F}_1, E) \cup (\tilde{F}_2, E)] \cup (\tilde{F}_3, E)$*and*
$(\tilde{F}_1, E) \cap [(\tilde{F}_2, E) \cap (\tilde{F}_3, E)] = [(\tilde{F}_1, E) \cap (\tilde{F}_2, E)] \cap (\tilde{F}_3, E)$*;*

(ii) $(\tilde{F}_1, E) \cup [(\tilde{F}_2, E) \cap (\tilde{F}_3, E)] = [(\tilde{F}_1, E) \cup (\tilde{F}_2, E)] \cap [(\tilde{F}_1, E) \cup (\tilde{F}_3, E)]$*and*
$(\tilde{F}_1, E) \cap [(\tilde{F}_2, E) \cup (\tilde{F}_3, E)] = [(\tilde{F}_1, E) \cap (\tilde{F}_2, E)] \cup [(\tilde{F}_1, E) \cap (\tilde{F}_3, E)]$*;*

(iii) $(\tilde{F}_1, E) \cup 0_{(X,E)} = (\tilde{F}_1, E)$*and*$(\tilde{F}_1, E) \cap 0_{(X,E)} = 0_{(X,E)}$*;*

(iv) $(\tilde{F}_1, E) \cup 1_{(X,E)} = (\tilde{F}_1, E)$*and*$(\tilde{F}_1, E) \cap 1_{(X,E)} = (\tilde{F}_1, E)$*;*

Proof. Obvious.

Proposition 2. *Let $(\tilde{F}_1, E)$ and $(\tilde{F}_2, E)$ be two complex single-valued neutrosophic soft sets over the universe set X. Then,*

(i) $[(\tilde{F}_1, E) \cup (\tilde{F}_2, E)]^c = (\tilde{F}_1, E)^c \cap (\tilde{F}_2, E)^c$

(ii) $[(\tilde{F}_1, E) \cap (\tilde{F}_2, E)]^c = (\tilde{F}_1, E)^c \cup (\tilde{F}_2, E)^c$

Proof. (i). For all $e \in E$ and $x \in X$,

$$\begin{aligned} (\tilde{F}_1, E) \cup (\tilde{F}_2, E) = \{\langle x, &\max\{T_{\tilde{F}_1(e)}(x), T_{\tilde{F}_2(e)}(x)\}, \max\{I_{\tilde{F}_1(e)}(x), I_{\tilde{F}_2(e)}(x)\}, \\ &\min\{F_{\tilde{F}_1(e)}(x), F_{\tilde{F}_2(e)}(x)\}\rangle\} \\ [(\tilde{F}_1, E) \cup (\tilde{F}_2, E)]^c = \{\langle x, &\min\{F_{\tilde{F}_1(e)}(x), F_{\tilde{F}_2(e)}(x)\}, 1 - \max\{I_{\tilde{F}_1(e)}(x), I_{\tilde{F}_2(e)}(x)\}, \\ &\max\{T_{\tilde{F}_1(e)}(x), T_{\tilde{F}_2(e)}(x)\}\rangle\} \end{aligned}$$

Now,

$$(\tilde{F}_1, E)^c = \{\langle x, F_{\tilde{F}_1(e)}(x), 1 - I_{\tilde{F}_1(e)}(x), T_{\tilde{F}_1(e)}(x)\rangle\}$$
$$(\tilde{F}_2, E)^c = \{\langle x, F_{\tilde{F}_2(e)}(x), 1 - I_{\tilde{F}_2(e)}(x), T_{\tilde{F}_2(e)}(x)\rangle\}$$

Then,

$$\begin{aligned}(\tilde{F}_1, E)^c \cap (\tilde{F}_2, E)^c &= \{\langle x, \min\{F_{\tilde{F}_1(e)}(x), F_{\tilde{F}_2(e)}(x)\}, \min\{1 - I_{\tilde{F}_1(e)}(x), 1 - I_{\tilde{F}_2(e)}(x)\},\\ &\quad \max\{T_{\tilde{F}_1(e)}(x), T_{\tilde{F}_2(e)}(x)\}\rangle\}\\ &= \{\langle x, \min\{F_{\tilde{F}_1(e)}(x), F_{\tilde{F}_2(e)}(x)\}, 1 - \max\{I_{\tilde{F}_1(e)}(x), I_{\tilde{F}_2(e)}(x)\},\\ &\quad \max\{T_{\tilde{F}_1(e)}(x), T_{\tilde{F}_2(e)}(x)\}\rangle\}\end{aligned}$$

Therefore, $[(\tilde{F}_1, E) \cup (\tilde{F}_2, E)]^c = (\tilde{F}_1, E)^c \cap (\tilde{F}_2, E)^c$.
(ii). It is obtained in a similar way.

Proposition 3. *Let* $(\tilde{F}_1, E)$ *and* $(\tilde{F}_2, E)$ *be two complex single-valued neutrosophic soft sets over the universe set* X*. Then,*

(i) $[(\tilde{F}_1, E) \vee (\tilde{F}_2, E)]^c = (\tilde{F}_1, E)^c \wedge (\tilde{F}_2, E)^c$

(ii) $[(\tilde{F}_1, E) \wedge (\tilde{F}_2, E)]^c = (\tilde{F}_1, E)^c \vee (\tilde{F}_2, E)^c$

Proof. (i). For all $e \in E$ *and* $x \in X$*,*

$$\begin{aligned}(\tilde{F}_1, E) \vee (\tilde{F}_2, E) &= \{\langle x, \max\{T_{\tilde{F}_1}(e)(x), T_{\tilde{F}_2}(e)(x)\}, \max\{I_{\tilde{F}_1}(e)(x), I_{\tilde{F}_2}(e)(x)\},\\ &\quad \min\{F_{\tilde{F}_1}(e)(x), F_{\tilde{F}_2}(e)(x)\}\rangle\}\\ [(\tilde{F}_1, E) \vee (\tilde{F}_2, E)]^c &= \{\langle x, \min\{F_{\tilde{F}_1}(e)(x), F_{\tilde{F}_2}(e)(x)\}, 1 - \max\{I_{\tilde{F}_1}(e)(x), I_{\tilde{F}_2}(e)(x)\},\\ &\quad \max\{T_{\tilde{F}_1}(e)(x), T_{\tilde{F}_2}(e)(x)\}\rangle\},\end{aligned}$$

On the other hand,

$$(\tilde{F}_1, E)^c = \{\langle x, F_{\tilde{F}_1}(e)(x), 1 - I_{\tilde{F}_1}(e)(x), RT_{\tilde{F}_1}(e)(x), T_{\tilde{F}_1}(e)(x)\rangle\}$$
$$(\tilde{F}_2, E)^c = \{\langle x, F_{\tilde{F}_2}(e)(x), 1 - I_{\tilde{F}_2}(e)(x), RT_{\tilde{F}_2}(e)(x), T_{\tilde{F}_2}(e)(x)\rangle\}$$

Then,

$$\begin{aligned}(\tilde{F}_1, E)^c \wedge (\tilde{F}_2, E)^c &= \{\langle x, \min\{F_{\tilde{F}_1}(e)(x), F_{\tilde{F}_2}(e)(x)\}, \min\{1 - I_{\tilde{F}_1}(e)(x), 1 - I_{\tilde{F}_2}(e)(x)\}\\ &\quad \max\{T_{\tilde{F}_1}(e)(x), T_{\tilde{F}_2}(e)(x)\}\rangle\}\\ &= \{\langle x, \min\{F_{\tilde{F}_1}(e)(x), F_{\tilde{F}_2}(e)(x)\}, 1 - \max\{I_{\tilde{F}_1}(e)(x), I_{\tilde{F}_2}(e)(x)\},\\ &\quad \max\{T_{\tilde{F}_1}(e)(x), T_{\tilde{F}_2}(e)(x)\}\rangle\},\end{aligned}$$

Therefore, $[(\tilde{F}_1, E) \vee (\tilde{F}_2, E)]^c = (\tilde{F}_1, E)^c \wedge (\tilde{F}_2, E)^c$.
(ii). It is obtained in a similar way.

Example 1. *Suppose that, the universe set X given by $X = \{x_1, x_2, x_3, x_4\}$ and the set of parameters $E = (e_1, e_2)$. Let us consider complex single-valued neutrosophic soft sets $(\tilde{F}_1, E) and (\tilde{F}_2, E)$ over the universe set X as follows*

$$(\tilde{F}_1, E) = \begin{bmatrix} e_1 = \langle x_1, 0.3e^{\iota\pi(0.2)}, 0.4e^{\iota\pi(0.3)}, 0.6e^{\iota\pi(0.5)}\rangle, \langle x_2, 0.4e^{\iota\pi(0.3)}, 0.2e^{\iota\pi(0.1)}, 0.8e^{\iota\pi(0.7)}\rangle, \\ \quad \langle x_3, 0.6e^{\iota\pi(0.5)}, 0.2e^{\iota\pi(0.1)}, 0.5e^{\iota\pi(0.4)}\rangle, \langle x_4, 0.2e^{\iota\pi(0.1)}, 0.3e^{\iota\pi(0.2)}, 0.4e^{\iota\pi(0.3)}\rangle \\ e_2 = \langle x_1, 0.4e^{\iota\pi(0.3)}, 0.3e^{\iota\pi(0.2)}, 0.8e^{\iota\pi(0.7)}\rangle, \langle x_2, 0.3e^{\iota\pi(0.2)}, 0.4e^{\iota\pi(0.3)}, 0.2e^{\iota\pi(0.1)}\rangle, \\ \quad \langle x_3, 0.3e^{\iota\pi(0.2)}, 0.2e^{\iota\pi(0.1)}, 0.7e^{\iota\pi(0.6)}\rangle, \langle x_4, 0.1e^{\iota\pi(0.1)}, 0.2e^{\iota\pi(0.1)}, 0.9e^{\iota\pi(0.8)}\rangle \end{bmatrix}$$

$$(\tilde{F}_2, E) = \begin{bmatrix} e_1 = \langle x_1, 0.6e^{\iota\pi(0.5)}, 0.3e^{\iota\pi(0.2)}, 0.8e^{\iota\pi(0.7)}\rangle, \langle x_2, 0.2e^{\iota\pi(0.1)}, 0.5e^{\iota\pi(0.4)}, 0.8e^{\iota\pi(0.7)}\rangle, \\ \quad \langle x_3, 0.1e^{\iota\pi(0.1)}, 0.1e^{\iota\pi(0.1)}, 0.4e^{\iota\pi(0.3)}\rangle, \langle x_4, 0.5e^{\iota\pi(0.4)}, 0.2e^{\iota\pi(0.1)}, 0.3e^{\iota\pi(0.2)}\rangle \\ e_2 = \langle x_1, 0.7e^{\iota\pi(0.6)}, 0.5e^{\iota\pi(0.4)}, 0.6e^{\iota\pi(0.5)}\rangle, \langle x_2, 0.4e^{\iota\pi(0.3)}, 0.2e^{\iota\pi(0.1)}, 0.3e^{\iota\pi(0.2)}\rangle, \\ \quad \langle x_3, 0.5e^{\iota\pi(0.4)}, 0.3e^{\iota\pi(0.2)}, 0.4e^{\iota\pi(0.3)}\rangle, \langle x_4, 0.4e^{\iota\pi(0.3)}, 0.2e^{\iota\pi(0.1)}, 0.6e^{\iota\pi(0.5)}\rangle \end{bmatrix}$$

Then, their union, intersection, AND, and OR operations are given as follows:

$$(\tilde{F}_1, E) \cup (\tilde{F}_2, E) = \begin{bmatrix} e_1 = \langle x_1, 0.6e^{\iota\pi(0.5)}, 0.4e^{\iota\pi(0.3)}, 0.6e^{\iota\pi(0.5)}\rangle, \langle x_2, 0.4e^{\iota\pi(0.3)}, 0.5e^{\iota\pi(0.4)}, 0.8e^{\iota\pi(0.7)}\rangle, \\ \quad \langle x_3, 0.6e^{\iota\pi(0.5)}, 0.2e^{\iota\pi(0.1)}, 0.4e^{\iota\pi(0.3)}\rangle, \langle x_4, 0.5e^{\iota\pi(0.4)}, 0.3e^{\iota\pi(0.2)}, 0.3e^{\iota\pi(0.2)}\rangle \\ e_2 = \langle x_1, 0.7e^{\iota\pi(0.6)}, 0.5e^{\iota\pi(0.4)}, 0.6e^{\iota\pi(0.5)}\rangle, \langle x_2, 0.4e^{\iota\pi(0.3)}, 0.4e^{\iota\pi(0.3)}, 0.2e^{\iota\pi(0.1)}\rangle, \\ \quad \langle x_3, 0.5e^{\iota\pi(0.4)}, 0.3e^{\iota\pi(0.2)}, 0.4e^{\iota\pi(0.3)}\rangle, \langle x_4, 0.4e^{\iota\pi(0.3)}, 0.2e^{\iota\pi(0.1)}, 0.6e^{\iota\pi(0.5)}\rangle \end{bmatrix}$$

$$(\tilde{F}_1, E) \cap (\tilde{F}, E) = \begin{bmatrix} e_1 = \langle x_1, 0.3e^{\iota\pi(0.2)}, 0.3e^{\iota\pi(0.3)}, 0.8e^{\iota\pi(0.7)}\rangle, \langle x_2, 0.2e^{\iota\pi(0.1)}, 0.2e^{\iota\pi(0.1)}, 0.8e^{\iota\pi(0.7)}\rangle, \\ \quad \langle x_3, 0.1e^{\iota\pi(0.1)}, 0.1e^{\iota\pi(0.1)}, 0.5e^{\iota\pi(0.4)}\rangle, \langle x_4, 0.2e^{\iota\pi(0.1)}, 0.2e^{\iota\pi(0.2)}, 0.4e^{\iota\pi(0.4)}\rangle \\ e_2 = \langle x_1, 0.3e^{\iota\pi(0.2)}, 0.3e^{\iota\pi(0.3)}, 0.8e^{\iota\pi(0.7)}\rangle, \langle x_2, 0.2e^{\iota\pi(0.1)}, 0.2e^{\iota\pi(0.1)}, 0.8e^{\iota\pi(0.7)}\rangle, \\ \quad \langle x_3, 0.1e^{\iota\pi(0.1)}, 0.1e^{\iota\pi(0.1)}, 0.5e^{\iota\pi(0.4)}\rangle, \langle x_4, 0.2e^{\iota\pi(0.1)}, 0.2e^{\iota\pi(0.2)}, 0.4e^{\iota\pi(0.3)}\rangle \end{bmatrix}$$

$$(\tilde{F}_1, E) \backslash (\tilde{F}_2, E) = \begin{bmatrix} e_1 = \langle x_1, 0.3e^{\iota\pi(0.2)}, 0.3e^{\iota\pi(0.2)}, 0.6e^{\iota\pi(0.5)}\rangle, \langle x_2, 0.4e^{\iota\pi(0.3)}, 0.2e^{\iota\pi(0.1)}, 0.8e^{\iota\pi(0.7)}\rangle, \\ \quad \langle x_3, 0.4e^{\iota\pi(0.3)}, 0.1e^{\iota\pi(0.1)}, 0.5e^{\iota\pi(0.4)}\rangle, \langle x_4, 0.2e^{\iota\pi(0.1)}, 0.2e^{\iota\pi(0.1)}, 0.5e^{\iota\pi(0.4)}\rangle \\ e_2 = \langle x_1, 0.4e^{\iota\pi(0.3)}, 0.3e^{\iota\pi(0.2)}, 0.8e^{\iota\pi(0.7)}\rangle, \langle x_2, 0.3e^{\iota\pi(0.2)}, 0.2e^{\iota\pi(0.1)}, 0.4e^{\iota\pi(0.3)}\rangle, \\ \quad \langle x_3, 0.3e^{\iota\pi(0.2)}, 0.2e^{\iota\pi(0.1)}, 0.7e^{\iota\pi(0.6)}\rangle, \langle x_4, 0.1e^{\iota\pi(0.1)}, 0.1e^{\iota\pi(0.1)}, 0.9e^{\iota\pi(0.8)}\rangle \end{bmatrix}$$

$$(\tilde{F}_1, E) \wedge (\tilde{F}, E) = \begin{bmatrix} (e_1, e_1) = \langle x_1, 0.3e^{\iota\pi(0.2)}, 0.3e^{\iota\pi(0.2)}, 0.8e^{\iota\pi(0.7)}\rangle, \langle x_2, 0.2e^{\iota\pi(0.1)}, 0.2e^{\iota\pi(0.1)}, 0.8e^{\iota\pi(0.7)}\rangle, \\ \quad \langle x_3, 0.1e^{\iota\pi(0.1)}, 0.1e^{\iota\pi(0.1)}, 0.5e^{\iota\pi(0.4)}\rangle, \langle x_4, 0.2e^{\iota\pi(0.1)}, 0.2e^{\iota\pi(0.1)}, 0.4e^{\iota\pi(0.3)}\rangle \\ (e_1, e_2) = \langle x_1, 0.3e^{\iota\pi(0.2)}, 0.4e^{\iota\pi(0.3)}, 0.6e^{\iota\pi(0.5)}\rangle, \langle x_2, 0.4e^{\iota\pi(0.3)}, 0.2e^{\iota\pi(0.1)}, 0.8e^{\iota\pi(0.7)}\rangle, \\ \quad \langle x_3, 0.5e^{\iota\pi(0.4)}, 0.2e^{\iota\pi(0.1)}, 0.5e^{\iota\pi(0.4)}\rangle, \langle x_4, 0.2e^{\iota\pi(0.1)}, 0.2e^{\iota\pi(0.1)}, 0.6e^{\iota\pi(0.5)}\rangle \\ (e_2, e_1) = \langle x_1, 0.4e^{\iota\pi(0.3)}, 0.3e^{\iota\pi(0.2)}, 0.8e^{\iota\pi(0.7)}\rangle, \langle x_2, 0.2e^{\iota\pi(0.1)}, 0.4e^{\iota\pi(0.3)}, 0.8e^{\iota\pi(0.7)}\rangle, \\ \quad \langle x_3, 0.1e^{\iota\pi(0.1)}, 0.1e^{\iota\pi(0.1)}, 0.7e^{\iota\pi(0.6)}\rangle, \langle x_4, 0.1e^{\iota\pi(0.1)}, 0.2e^{\iota\pi(0.1)}, 0.9e^{\iota\pi(0.8)}\rangle \\ (e_2, e_2) = \langle x_1, 0.3e^{\iota\pi(0.2)}, 0.3e^{\iota\pi(0.2)}, 0.8e^{\iota\pi(0.7)}\rangle, \langle x_2, 0.2e^{\iota\pi(0.1)}, 0.2e^{\iota\pi(0.1)}, 0.8e^{\iota\pi(0.7)}\rangle, \\ \quad \langle x_3, 0.1e^{\iota\pi(0.1)}, 0.1e^{\iota\pi(0.1)}, 0.5e^{\iota\pi(0.4)}\rangle, \langle x_4, 0.2e^{\iota\pi(0.1)}, 0.2e^{\iota\pi(0.1)}, 0.4e^{\iota\pi(0.3)}\rangle \end{bmatrix}$$

$$(\tilde{F}_1, E)\vee(\tilde{F}, E) = \begin{bmatrix} (e_1, e_1) = \langle x_1, 0.6e^{\iota\pi(0.5)}, 0.4e^{\iota\pi(0.3)}, 0.6e^{\iota\pi(0.5)}\rangle, \langle x_2, 0.4e^{\iota\pi(0.3)}, 0.5e^{\iota\pi(0.4)}, 0.8e^{\iota\pi(0.7)}\rangle, \\ \langle x_3, 0.6e^{\iota\pi(0.5)}, 0.2e^{\iota\pi(0.1)}, 0.4e^{\iota\pi(0.3)}\rangle, \langle x_4, 0.5e^{\iota\pi(0.4)}, 0.3e^{\iota\pi(0.2)}, 0.3e^{\iota\pi(0.2)}\rangle \\ (e_1, e_2) = \langle x_1, 0.7e^{\iota\pi(0.6)}, 0.5e^{\iota\pi(0.4)}, 0.8e^{\iota\pi(0.7)}\rangle, \langle x_2, 0.4e^{\iota\pi(0.3)}, 0.2e^{\iota\pi(0.1)}, 0.3e^{\iota\pi(0.2)}\rangle, \\ \langle x_3, 0.6e^{\iota\pi(0.5)}, 0.3e^{\iota\pi(0.2)}, 0.4e^{\iota\pi(0.3)}\rangle, \langle x_4, 0.4e^{\iota\pi(0.3)}, 0.3e^{\iota\pi(0.2)}, 0.4e^{\iota\pi(0.3)}\rangle \\ (e_2, e_1) = \langle x_1, 0.6e^{\iota\pi(0.5)}, 0.3e^{\iota\pi(0.2)}, 0.8e^{\iota\pi(0.7)}\rangle, \langle x_2, 0.3e^{\iota\pi(0.2)}, 0.5e^{\iota\pi(0.4)}, 0.2e^{\iota\pi(0.1)}\rangle, \\ \langle x_3, 0.3e^{\iota\pi(0.2)}, 0.2e^{\iota\pi(0.1)}, 0.4e^{\iota\pi(0.3)}\rangle, \langle x_4, 0.5e^{\iota\pi(0.4)}, 0.2e^{\iota\pi(0.1)}, 0.3e^{\iota\pi(0.2)}\rangle \\ (e_2, e_2) = \langle x_1, 0.7e^{\iota\pi(0.6)}, 0.5e^{\iota\pi(0.4)}, 0.6e^{\iota\pi(0.5)}\rangle, \langle x_2, 0.4e^{\iota\pi(0.3)}, 0.4e^{\iota\pi(0.3)}, 0.2e^{\iota\pi(0.1)}\rangle, \\ \langle x_3, 0.5e^{\iota\pi(0.4)}, 0.3e^{\iota\pi(0.2)}, 0.4e^{\iota\pi(0.3)}\rangle, \langle x_4, 0.4e^{\iota\pi(0.3)}, 0.2e^{\iota\pi(0.1)}, 0.6e^{\iota\pi(0.5)}\rangle \end{bmatrix}$$

4. Complex Single-Valued Neutrosophic Soft Topological Spaces

In this section, we introduced the complex single-valued neutrosophic soft topology based on the defined operations of the complex single-valued neutrosophic soft union, intersection, the neutrosophic soft null and absolute sets. Some examples are given for better understanding the concepts.

Definition 14. *Let $CSVNSS(X, E)$ be the family of all complex single-valued neutrosophic soft sets over the universe set X and $\tau \subset CSVNSS(X, E)$. Then τ is said to be a complex single-valued neutrosophic soft topology on X if*

(i) $0_{(X,E)}$ *and* $1_{(X,E)} \in \tau$,

(ii) The union of any number of complex single-valued neutrosophic soft sets in $\tau \in \tau$,

(iii) The intersection of a finite number of complex single-valued neutrosophic soft sets in $\tau \in \tau$.

Then, (X, τ, E) is said to be a complex single-valued neutrosophic soft topological space (CSVNSTS) over X. Each members of τ is said to be complex single-valued neutrosophic soft open set.

Definition 15. *Let (X, τ, E) be a complex single-valued neutrosophic soft topological space over X and $(\tilde{F}, E)$ be a complex single-valued neutrosophic soft set over X . Then $(\tilde{F}, E)$ is said to be complex single-valued neutrosophic soft closed set iff its complement is a complex single-valued neutrosophic soft open set.*

Proposition 4. *Let (X, τ, E) be a complex single-valued neutrosophic soft topological space over the universe set X. Then,*

(i) $0_{(X,E)}$ *and* $1_{(X,E)}$ *are complex single-valued neutrosophic soft closed sets over X,*

(ii) The union of any number of complex single-valued neutrosophic soft sets is a complex single-valued neutrosophic soft closed sets over X,

(iii) The intersection of a finite number of complex single-valued neutrosophic soft sets is a complex single-valued neutrosophic soft closed sets over X.

Definition 16. *Let $CSVNSS(X, E)$ be the family of all complex single-valued neutrosophic soft sets over the universe set X.*

(i) If $\tau = \{0_{(X,E)}, 1_{(X,E)}\}$, then τ is said to be complex single-valued neutrosophic soft indiscrete topology and (X, τ, E) is said to be a complex single-valued neutrosophic soft indiscrete topological space over X.

(ii) If $\tau = CSVNSS(X, E)$, then τ is said to be complex single-valued neutrosophic soft discrete topology and (X, τ, E) is said to be a complex single-valued neutrosophic soft discrete topological space over X.

Proposition 5. *Let (X, τ_1, E) and (X, τ_2, E) be two complex single-valued neutrosophic soft topological space over the same universe set X. Then $(X, \tau_1 \cap \tau_2, E)$ is a complex single-valued neutrosophic soft topological space over X.*

Proof. (i). Since $0_{(X,E)}$, $1_{(X,E)} \in \tau_1$ and $0_{(X,E)}$, $1_{(X,E)} \in \tau_2$, then $0_{(X,E)}$, $1_{(X,E)} \in \tau_1 \cap \tau_2$.
(ii). Suppose that $\{(\tilde{F}_i, E)|i \in I\}$ be a family of complex double-valued neutrosophic soft sets in $\tau_1 \cap \tau_2$.
Then $(\tilde{F}_i, E) \in \tau_1$ and $(\tilde{F}_i, E) \in \tau_2$ for all $i \in I$, so $\cup_{i\in I}(\tilde{F}_i, E) \in \tau_1$ and $\cup_{i\in I}(\tilde{F}_i, E) \in \tau_2$. Thus $\cup_{i\in I}(\tilde{F}_i, E) \in \tau_1 \cap \tau_2$. (iii). Let $\{(\tilde{F}_i, E)|i = \overline{1, n}\}$ be a family of finite number of complex single-valued neutrosophic soft sets in $\tau_1 \cap \tau_2$.
Then $(\tilde{F}_i, E) \in \tau_1$ and $(\tilde{F}_i, E) \in \tau_2$ for all $i = \overline{1, n}$, so $\bigcap_{i=I}^{n}(\tilde{F}_i, E) \in \tau_1$ and $\bigcap_{i=I}^{n}(\tilde{F}_i, E) \in \tau_2$. Thus $\bigcap_{i=I}^{n}(\tilde{F}_i, E) \in \tau_1 \cap \tau_2$.

Remark 1. *The union of two complex single-valued neutrosophic soft topologies over X may not be a complex single-valued neutrosophic soft topology on X.*

Example 2. *Let $X = \{x_1, x_2, x_3\}$ be an initial universe set, $E = \{e_1, e_2\}$ be a set of parameters and:*

$$\tau_1 = \{0_{(X,E)}, 1_{(X,E)}, (\tilde{F}_1, E), (\tilde{F}_2, E), (\tilde{F}_3, E)\},$$
$$\tau_2 = \{0_{(X,E)}, 1_{(X,E)}, (\tilde{F}_2, E), (\tilde{F}_4, E)\}.$$

be two complex single-valued neutrosophic soft topologies over X. Here, the complex single-valued neutrosophic soft sets $(\tilde{F}_1, E)$, $(\tilde{F}_2, E)$, $(\tilde{F}_3, E)$ and $(\tilde{F}_4, E)$ are defined as follows:

$$(\tilde{F}_1, E) = \begin{bmatrix} e_1 = \langle x_1, 0.9e^{\iota\pi(0.9)}, 0.6e^{\iota\pi(0.8)}, 0.3e^{\iota\pi(0.5)}\rangle, \langle x_2, 0.7e^{\iota\pi(0.7)}, 0.6e^{\iota\pi(0.5)}, 0.5e^{\iota\pi(0.4)}\rangle \\ \quad \langle x_3, 0.4e^{\iota\pi(0.3)}, 0.5e^{\iota\pi(0.2)}, 0.4e^{\iota\pi(0.2)}\rangle; \\ e_2 = \langle x_1, 0.7e^{\iota\pi(0.9)}, 0.3e^{\iota\pi(0.8)}, 0.4e^{\iota\pi(0.7)}\rangle, \langle x_2, 0.6e^{\iota\pi(0.5)}, 0.5e^{\iota\pi(0.7)}, 0.4e^{\iota\pi(0.2)}\rangle, \\ \quad \langle x_3, 0.7e^{\iota\pi(0.8)}, 0.4e^{\iota\pi(0.4)}, 0.3e^{\iota\pi(0.4)}\rangle. \end{bmatrix}$$

$$(\tilde{F}_2, E) = \begin{bmatrix} e_1 = \langle x_1, 0.7e^{\iota\pi(0.8)}, 0.5e^{\iota\pi(0.4)}, 0.5e^{\iota\pi(0.5)}\rangle, \langle x_2, 0.6e^{\iota\pi(0.4)}, 0.5e^{\iota\pi(0.5)}, 0.7e^{\iota\pi(0.6)}\rangle \\ \quad \langle x_3, 0.3e^{\iota\pi(0.2)}, 0.4e^{\iota\pi(0.2)}, 0.6e^{\iota\pi(0.8)}\rangle; \\ e_2 = \langle x_1, 0.6e^{\iota\pi(0.6)}, 0.2e^{\iota\pi(0.6)}, 0.5e^{\iota\pi(0.7)}\rangle, \langle x_2, 0.5e^{\iota\pi(0.4)}, 0.4e^{\iota\pi(0.1)}, 0.6e^{\iota\pi(0.7)}\rangle, \\ \quad \langle x_3, 0.4e^{\iota\pi(0.3)}, 0.3e^{\iota\pi(0.3)}, 0.5e^{\iota\pi(0.4)}\rangle. \end{bmatrix}$$

$$(\tilde{F}_3, E) = \begin{bmatrix} e_1 = \langle x_1, 0.5e^{\iota\pi(0.6)}, 0.4e^{\iota\pi(0.2)}, 0.6e^{\iota\pi(0.5)}\rangle, \langle x_2, 0.4e^{\iota\pi(0.2)}, 0.3e^{\iota\pi(0.1)}, 0.7e^{\iota\pi(0.7)}\rangle \\ \quad \langle x_3, 0.2e^{\iota\pi(0.1)}, 0.3e^{\iota\pi(0.2)}, 0.8e^{\iota\pi(0.9)}\rangle; \\ e_2 = \langle x_1, 0.4e^{\iota\pi(0.3)}, 0.2e^{\iota\pi(0.1)}, 0.6e^{\iota\pi(0.8)}\rangle, \langle x_2, 0.4e^{\iota\pi(0.3)}, 0.2e^{\iota\pi(0.1)}, 0.8e^{\iota\pi(0.9)}\rangle, \\ \quad \langle x_3, 0.3e^{\iota\pi(0.2)}, 0.3e^{\iota\pi(0.1)}, 0.6e^{\iota\pi(0.5)}\rangle. \end{bmatrix}$$

$$(\tilde{F}_4, E) = \begin{bmatrix} e_1 = \langle x_1, 0.6e^{\iota\pi(0.7)}, 0.3e^{\iota\pi(0.2)}, 0.2e^{\iota\pi(0.1)}\rangle, \langle x_2, 0.5e^{\iota\pi(0.4)}, 0.3e^{\iota\pi(0.3)}, 0.8e^{\iota\pi(0.9)}\rangle \\ \quad \langle x_3, 0.2e^{\iota\pi(0.2)}, 0.3e^{\iota\pi(0.1)}, 0.9e^{\iota\pi(0.9)}\rangle; \\ e_2 = \langle x_1, 0.3e^{\iota\pi(0.3)}, 0.2e^{\iota\pi(0.1)}, 0.7e^{\iota\pi(0.8)}\rangle, \langle x_2, 0.4e^{\iota\pi(0.2)}, 0.1e^{\iota\pi(0.1)}, 0.9e^{\iota\pi(0.9)}\rangle, \\ \quad \langle x_3, 0.2e^{\iota\pi(0.2)}, 0.2e^{\iota\pi(0.1)}, 0.7e^{\iota\pi(0.8)}\rangle. \end{bmatrix}$$

Since $(\tilde{F}_1, E) \cup (\tilde{F}_4, E) \notin \tau_1 \cup \tau_2$, then $\tau_1 \cup \tau_2$ is not a complex single-valued neutrosophic soft topology over X.

Proposition 6. *Let (X, τ, E) be a complex single-valued neutrosophic soft topological space over X and*

$$\tau = \{(\tilde{F}_i, E) : (\tilde{F}_i, E) \in CSVNSS(X, E)\} = \{[e, \tilde{F}_i(e)]_{e\in E} : (\tilde{F}_i, E) \in CSVNSS(X, E)\}$$

where $\tilde{F}_i(e) = \{\langle x, T_{\tilde{F}_i(e)}(x), I_{\tilde{F}_i(e)}(x), F_{\tilde{F}_i(e)}(x)\rangle : x \in X\}$. Then

$$\tau_1 = \{[T_{\tilde{F}_i(e)}(X)]_{e\in E}\}$$
$$\tau_2 = \{[I_{\tilde{F}_i(e)}(X)]_{e\in E}\}$$
$$\tau_3 = \{[F_{\tilde{F}_i(e)}(X)]_{e\in E}\}$$

define complex fuzzy soft topologies on X.

Proof. (i). $0_{(X,E)}, 1_{(X,E)} \in \tau \Rightarrow 0, 1 \in \tau_1, 0, 1 \in \tau_2, 0, 1 \in \tau_3 and 0, 1 \in \tau_4$. *(ii). Suppose that $(\tilde{F}_i, E)|i \in I$ be a family of complex single-valued neutrosophic soft sets in τ. Then $\{[T_{\tilde{F}_i(e)}(X)]_{e\in E}\}_{i\in I}$ is a family of complex fuzzy soft sets in τ_1, $\{[I_{\tilde{F}_i(e)}(X)]_{e\in E}\}_{i\in I}$ is a family of complex fuzzy soft sets in τ_2, $\{[F_{\tilde{F}_i(e)}(X)]_{e\in E}\}_{i\in I}$ is a family of complex fuzzy soft sets in τ_3. Since τ is a complex single-valued neutrosophic soft topology, then $\cup_{i\in I}(\tilde{F}_i, E) \in \tau_1$. That is,*

$$\cup_{i\in I}(\tilde{F}_i, E) = \{\langle sup[T_{\tilde{F}_i(e)}(X)]_{e\in E}, sup[I_{\tilde{F}_i(e)}(X)]_{e\in E}, inf[F_{\tilde{F}_i(e)}(X)]_{e\in E}\rangle\}_{i\in I} \in \tau.$$

Therefore,

$$\{sup[T_{\tilde{F}_i(e)}(X)]_{e\in E}\}_{i\in I} \in \tau_1$$
$$\{sup[I_{\tilde{F}_i(e)}(X)]_{e\in E}\}_{i\in I} \in \tau_2$$
$$\{inf[F_{\tilde{F}_i(e)}(X)]_{e\in E}\}_{i\in I} \in \tau_3.$$

(iii). Suppose $\{(\tilde{F}_i, E)|i = \overline{1, n}\}$ be a family of finite number of complex single-valued neutrosophic soft sets in τ.
Then $\{[T_{\tilde{F}_i(e)}(X)]_{e\in E}\}_{i=\overline{1,n}}$ is a family of complex fuzzy soft sets in τ_1, $\{[I_{\tilde{F}_i(e)}(X)]_{e\in E}\}_{i=\overline{1,n}}$ is a family of complex fuzzy soft sets in τ_2, $\{[F_{\tilde{F}_i(e)}(X)]_{e\in E}\}_{i=\overline{1,n}}$ is a family of complex fuzzy soft sets in τ_3. Since τ is a complex single-valued neutrosophic soft topology, then $\cap_{i=1}^{n}(\tilde{F}_i, E) \in \tau_1$. That is,

$$\cap_{i=1}^{n}(\tilde{F}_i, E) = \{\langle \min[T_{\tilde{F}_i(e)}(X)]_{e\in E}, \min[I_{\tilde{F}_i(e)}(X)]_{e\in E}, \max[F_{\tilde{F}_i(e)}(X)]_{e\in E}\rangle\}_{i=\overline{1,n}} \in \tau.$$

Therefore,

$$\{\min[T_{\tilde{F}_i(e)}(X)]_{e\in E}\}_{i\in I} \in \tau_1$$
$$\{\min[I_{\tilde{F}_i(e)}(X)]_{e\in E}\}_{i\in I} \in \tau_2$$
$$\{\min[F_{\tilde{F}_i(e)}(X)]^c_{e\in E}\}_{i\in I} \in \tau_3.$$

This completes the proof.

Remark 2. *Generally, converse of the above proposition is not true.*

Example 3. *Let $X = \{x_1, x_2, x_3\}$ be an initial universe set, $E = \{e_1, e_2\}$ be a set of parameters and:*

$$\tau_1 = \{0_{(X,E)}, 1_{(X,E)}, (\tilde{F}_1, E), (\tilde{F}_2, E), (\tilde{F}_3, E)\}$$

be a family of complex single-valued neutrosophic soft sets over X. Here, the complex single-valued neutrosophic soft sets $(\tilde{F}_1, E)$, $(\tilde{F}_2, E)$ and $(\tilde{F}_3, E)$ are defined as follows:

$$(\tilde{F}_1, E) = \begin{bmatrix} e_1 = \langle x_1, 0.9e^{\iota\pi(0.9)}, 0.6e^{\iota\pi(0.8)}, 0.3e^{\iota\pi(0.7)}\rangle, \langle x_2, 0.7e^{\iota\pi(0.7)}, 0.6e^{\iota\pi(0.5)}, 0.5e^{\iota\pi(0.4)}\rangle \\ \quad \langle x_3, 0.4e^{\iota\pi(0.3)}, 0.5e^{\iota\pi(0.2)}, 0.4e^{\iota\pi(0.2)}\rangle; \\ e_2 = \langle x_1, 0.7e^{\iota\pi(0.9)}, 0.3e^{\iota\pi(0.8)}, 0.4e^{\iota\pi(0.7)}\rangle, \langle x_2, 0.6e^{\iota\pi(0.5)}, 0.5e^{\iota\pi(0.7)}, 0.4e^{\iota\pi(0.2)}\rangle, \\ \quad \langle x_3, 0.7e^{\iota\pi(0.8)}, 0.4e^{\iota\pi(0.4)}, 0.3e^{\iota\pi(0.4)}\rangle. \end{bmatrix}$$

$$(\tilde{F}_2, E) = \begin{bmatrix} e_1 = \langle x_1, 0.7e^{\iota\pi(0.8)}, 0.5e^{\iota\pi(0.4)}, 0.5e^{\iota\pi(0.8)}\rangle, \langle x_2, 0.6e^{\iota\pi(0.4)}, 0.5e^{\iota\pi(0.5)}, 0.7e^{\iota\pi(0.6)}\rangle \\ \quad \langle x_3, 0.3e^{\iota\pi(0.2)}, 0.4e^{\iota\pi(0.2)}, 0.6e^{\iota\pi(0.8)}\rangle; \\ e_2 = \langle x_1, 0.6e^{\iota\pi(0.6)}, 0.2e^{\iota\pi(0.6)}, 0.5e^{\iota\pi(0.8)}\rangle, \langle x_2, 0.5e^{\iota\pi(0.4)}, 0.4e^{\iota\pi(0.1)}, 0.6e^{\iota\pi(0.7)}\rangle, \\ \quad \langle x_3, 0.4e^{\iota\pi(0.3)}, 0.3e^{\iota\pi(0.3)}, 0.5e^{\iota\pi(0.4)}\rangle. \end{bmatrix}$$

$$(\tilde{F}_3, E) = \begin{bmatrix} e_1 = \langle x_1, 0.8e^{\iota\pi(0.8)}, 0.4e^{\iota\pi(0.2)}, 0.6e^{\iota\pi(0.8)}\rangle, \langle x_2, 0.4e^{\iota\pi(0.2)}, 0.3e^{\iota\pi(0.1)}, 0.7e^{\iota\pi(0.7)}\rangle \\ \quad \langle x_3, 0.2e^{\iota\pi(0.1)}, 0.3e^{\iota\pi(0.2)}, 0.8e^{\iota\pi(0.9)}\rangle; \\ e_2 = \langle x_1, 0.4e^{\iota\pi(0.3)}, 0.2e^{\iota\pi(0.1)}, 0.6e^{\iota\pi(0.8)}\rangle, \langle x_2, 0.4e^{\iota\pi(0.3)}, 0.2e^{\iota\pi(0.1)}, 0.8e^{\iota\pi(0.9)}\rangle, \\ \quad \langle x_3, 0.3e^{\iota\pi(0.2)}, 0.3e^{\iota\pi(0.1)}, 0.6e^{\iota\pi(0.5)}\rangle. \end{bmatrix}$$

Then,

$$\tau_1 = \{\langle T_{\tilde{F}_{0_{(X,E)^{(e)}}}}(X), T_{\tilde{F}_{1_{(X,E)^{(e)}}}}(X), T_{\tilde{F}_1(e)}(X), T_{\tilde{F}_2(e)}(X), T_{\tilde{F}_3(e)}(X)\rangle_{e\in E}\},$$
$$\tau_2 = \{\langle I_{\tilde{F}_{0_{(X,E)^{(e)}}}}(X), I_{\tilde{F}_{1_{(X,E)^{(e)}}}}(X), I_{\tilde{F}_1(e)}(X), I_{\tilde{F}_2(e)}(X), I_{\tilde{F}_3(e)}(X)\rangle_{e\in E}\},$$
$$\tau_3 = \{\langle F_{\tilde{F}_{0_{(X,E)^{(e)}}}}(X), F_{\tilde{F}_{1_{(X,E)^{(e)}}}}(X), F_{\tilde{F}_1(e)}(X), F_{\tilde{F}_2(e)}(X), F_{\tilde{F}_3(e)}(X)\rangle_{e\in E}\}.$$

are complex fuzzy soft topologies on X. For example,

$$\begin{aligned} \tau_1 = \{&\langle (0,0,0), (1,1,1), (0.9e^{\iota\pi(0.9)}, 0.7e^{\iota\pi(0.7)}, 0.4e^{\iota\pi(0.3)}), \\ &(0.7e^{\iota\pi(0.8)}, 0.6e^{\iota\pi(0.4)}, 0.3e^{\iota\pi(0.2)}), (0.8e^{\iota\pi(0.8)}, 0.4e^{\iota\pi(0.2)}, 0.2e^{\iota\pi(0.1)})\rangle_{e_1}, \\ &\langle (0,0,0), (1,1,1), (0.7e^{\iota\pi(0.9)}, 0.6e^{\iota\pi(0.5)}, 0.7e^{\iota\pi(0.8)}), \\ &(0.6e^{\iota\pi(0.6)}, 0.5e^{\iota\pi(0.4)}, 0.4e^{\iota\pi(0.3)}), (0.4e^{\iota\pi(0.3)}, 0.4e^{\iota\pi(0.3)}, 0.3e^{\iota\pi(0.2)})\rangle_{e_2}\} \end{aligned}$$

$$\begin{aligned} \tau_2 = \{&\langle (0,0,0), (1,1,1), (0.6e^{\iota\pi(0.8)}, 0.6e^{\iota\pi(0.5)}, 0.5e^{\iota\pi(0.2)}), \\ &(0.5e^{\iota\pi(0.4)}, 0.5e^{\iota\pi(0.5)}, 0.4e^{\iota\pi(0.2)}), (0.4e^{\iota\pi(0.2)}, 0.3e^{\iota\pi(0.1)}, 0.3e^{\iota\pi(0.2)})\rangle_{e_1}, \\ &\langle (0,0,0), (1,1,1), (0.3e^{\iota\pi(0.8)}, 0.5e^{\iota\pi(0.7)}, 0.4e^{\iota\pi(0.4)}), \\ &(0.2e^{\iota\pi(0.6)}, 0.4e^{\iota\pi(0.1)}, 0.3e^{\iota\pi(0.3)}), (0.2e^{\iota\pi(0.1)}, 0.2e^{\iota\pi(0.1)}, 0.3e^{\iota\pi(0.1)})\rangle_{e_2}\} \end{aligned}$$

$$\begin{aligned} \tau_3 = \{&\langle (0,0,0), (1,1,1), (0.3e^{\iota\pi(0.7)}, 0.5e^{\iota\pi(0.4)}, 0.4e^{\iota\pi(0.2)}), \\ &(0.5e^{\iota\pi(0.8)}, 0.7e^{\iota\pi(0.6)}, 0.6e^{\iota\pi(0.8)}), (0.6e^{\iota\pi(0.8)}, 0.7e^{\iota\pi(0.7)}, 0.8e^{\iota\pi(0.9)})\rangle_{e_1}, \\ &\langle (0,0,0), (1,1,1), (0.4e^{\iota\pi(0.7)}, 0.4e^{\iota\pi(0.2)}, 0.3e^{\iota\pi(0.4)}), \\ &(0.5e^{\iota\pi(0.8)}, 0.6e^{\iota\pi(0.7)}, 0.5e^{\iota\pi(0.4)}), (0.6e^{\iota\pi(0.8)}, 0.8e^{\iota\pi(0.9)}, 0.6e^{\iota\pi(0.5)})\rangle_{e_2}\} \end{aligned}$$

Since $(\tilde{F}_2, E) \cap (\tilde{F}_3, E) \notin \tau$, τ is not a complex single-valued neutrosophic soft topology on X.

Proposition 7. *Let (X, τ, E) be a complex single-valued neutrosophic soft topological space over X. Then*

$$\tau_{1_e} = \{[T_{\tilde{F}(e)}(X)] : \tilde{F}, E \in \tau\}$$
$$\tau_{2_e} = \{[I_{\tilde{F}(e)}(X)] : \tilde{F}, E \in \tau\}$$
$$\tau_{3_e} = \{[F_{\tilde{F}(e)}(X)] : \tilde{F}, E \in \tau\}$$

for each $e \in E$ define complex fuzzy topologies on X.

Remark 3. *Generally converse of the above proposition is not true.*

Example 4. *Let us consider the Example* 3. *Then,*

$$\tau_{1_{e_1}} = \{\langle T_{\tilde{F}_{0_{(X,E)}(e_1)}}(X), T_{\tilde{F}_{1_{(X,E)}(e_1)}}(X), T_{\tilde{F}_1(e_1)}(X), T_{\tilde{F}_2(e_1)}(X), T_{\tilde{F}_3(e_1)}(X)\rangle\},$$
$$\tau_{2_{e_1}} = \{\langle I_{\tilde{F}_{0_{(X,E)}(e_1)}}(X), I_{\tilde{F}_{1_{(X,E)}(e_1)}}(X), I_{\tilde{F}_1(e_1)}(X), I_{\tilde{F}_2(e_1)}(X), I_{\tilde{F}_3(e_1)}(X)\rangle\},$$
$$\tau_{3_{e_1}} = \{\langle F_{\tilde{F}_{0_{(X,E)}(e_1)}}(X), F_{\tilde{F}_{1_{(X,E)}(e_1)}}(X), F_{\tilde{F}_1(e_1)}(X), F_{\tilde{F}_2(e_1)}(X), F_{\tilde{F}_3(e_1)}(X)\rangle\}.$$

are complex fuzzy soft topologies on X. For example,

$$\tau_{1_{e_1}} = \{\langle(0,0,0),(1,1,1),(0.9e^{\iota\pi(0.9)}, 0.7e^{\iota\pi(0.7)}, 0.4e^{\iota\pi(0.3)}),$$
$$(0.7e^{\iota\pi(0.8)}, 0.6e^{\iota\pi(0.4)}, 0.3e^{\iota\pi(0.2)}), (0.8e^{\iota\pi(0.8)}, 0.4e^{\iota\pi(0.2)}, 0.2e^{\iota\pi(0.1)})\rangle\}$$

$$\tau_{2_{e_1}} = \{\langle(0,0,0),(1,1,1),(0.6e^{\iota\pi(0.8)}, 0.6e^{\iota\pi(0.5)}, 0.5e^{\iota\pi(0.2)}),$$
$$(0.5e^{\iota\pi(0.4)}, 0.5e^{\iota\pi(0.5)}, 0.4e^{\iota\pi(0.2)}), (0.4e^{\iota\pi(0.2)}, 0.3e^{\iota\pi(0.1)}, 0.3e^{\iota\pi(0.2)})\rangle\}$$

$$\tau_{3_{e_1}} = \{\langle(0,0,0),(1,1,1),(0.3e^{\iota\pi(0.7)}, 0.5e^{\iota\pi(0.4)}, 0.4e^{\iota\pi(0.2)}),$$
$$(0.5e^{\iota\pi(0.8)}, 0.7e^{\iota\pi(0.6)}, 0.6e^{\iota\pi(0.8)}), (0.6e^{\iota\pi(0.8)}, 0.7e^{\iota\pi(0.7)}, 0.8e^{\iota\pi(0.9)})\rangle\}$$

Here, $\{\tau_{1_{e_1}}, \tau_{2_{e_1}}, \tau_{3_{e_1}}\}$ and $\{\tau_{1_{e_2}}, \tau_{2_{e_2}}, \tau_{3_{e_2}}\}$ are complex fuzzy quadri-topology on X. But τ is not a complex single-valued neutrosophic soft topology on X.

Definition 17. *Let (X, τ, E) be a complex single-valued neutrosophic soft topological space over X and $(\tilde{F}, E) \in CSVNSS(X, E)$ be a complex single-valued neutrosophic soft set. Then, the complex single-valued neutrosophic soft interior of $(\tilde{F}, E)$, denoted by $(\tilde{F}, E)^\circ$ is defined as the complex single-valued neutrosophic soft union of all the complex single-valued neutrosophic soft open subsets of $(\tilde{F}, E)$.*
Clearly $(\tilde{F}, E)^\circ$ is biggest complex single-valued neutrosophic soft open set that is contained by $(\tilde{F}, E)$.

Example 5. *Let us consider the complex single-valued neutrosophic soft topology τ_1 given in Example* 2.*Suppose that an any $(\tilde{F}, E) \in CSVNSS(X, E)$ is defined as following:*

$$(\tilde{F}, E) = \begin{bmatrix} e_1 = \langle x_1, 0.8e^{\iota\pi(0.9)}, 0.6e^{\iota\pi(0.8)}, 0.4e^{\iota\pi(0.3)}\rangle, \langle x_2, 0.7e^{\iota\pi(0.6)}, 0.9e^{\iota\pi(0.8)}, 0.3e^{\iota\pi(0.2)}\rangle \\ \quad \langle x_3, 0.5e^{\iota\pi(0.3)}, 0.6e^{\iota\pi(0.7)}, 0.3e^{\iota\pi(0.2)}\rangle; \\ e_2 = \langle x_1, 0.8e^{\iota\pi(0.7)}, 0.7e^{\iota\pi(0.6)}, 0.2e^{\iota\pi(0.3)}\rangle, \langle x_2, 0.9e^{\iota\pi(0.7)}, 0.7e^{\iota\pi(0.7)}, 0.4e^{\iota\pi(0.3)}\rangle, \\ \quad \langle x_3, 0.8e^{\iota\pi(0.7)}, 0.5e^{\iota\pi(0.6)}, 0.4e^{\iota\pi(0.3)}\rangle. \end{bmatrix}$$

Then $0_{(X,E)}, (\tilde{F}_2, E), (\tilde{F}_3, E) \subseteq (\tilde{F}, E)$. Therefore, $(\tilde{F}, E)^\circ = 0_{(X,E)} \cup (\tilde{F}_2, E) \cup (\tilde{F}_3, E) = (\tilde{F}, E)$.

Theorem 1. *Let (X, τ, E) be a complex single-valued neutrosophic soft topological space over X and $(\tilde{F}, E) \in CSVNSS(X, E)$. $(\tilde{F}, E)$ is a complex single-valued neutrosophic soft open set and iff $(\tilde{F}, E) = (\tilde{F}, E)^{\circ}$.*

Proof. Let $(\tilde{F}, E)$ be a complex single-valued neutrosophic soft open set. Then the biggest complex single-valued neutrosophic soft open set that is contained by $(\tilde{F}, E)$ is equal to $(\tilde{F}, E)$. Hence, $(\tilde{F}, E) = (\tilde{F}, E)^{\circ}$
Conversely, it is known that $(\tilde{F}, E)^{\circ}$ is a complex single-valued neutrosophic soft open set and if $(\tilde{F}, E) = (\tilde{F}, E)^{\circ}$, then $(\tilde{F}, E)$ is a complex single-valued neutrosophic soft open set.

Theorem 2. *Let (X, τ, E) be a complex single-valued neutrosophic soft topological space over X and $(\tilde{F}_1, E), (\tilde{F}_2, E) \in CSVNSS(X, E)$. Then,*

(i) $[(\tilde{F}, E)^{\circ}]^{\circ} = (\tilde{F}, E)^{\circ}$,

(ii) $(0_{(X,E)})^{\circ} = 0_{(X,E)}$ *and* $(1_{(X,E)})^{\circ} = 1_{(X,E)}$,

(iii) $(\tilde{F}_1, E) \subseteq (\tilde{F}_2, E) \Rightarrow (\tilde{F}_1, E)^{\circ} \subseteq (\tilde{F}_2, E)^{\circ}$,

(iv) $[(\tilde{F}_1, E) \cap (\tilde{F}_2, E)]^{\circ} = (\tilde{F}_1, E)^{\circ} \cap (\tilde{F}_2, E)^{\circ}$,

(v) $(\tilde{F}_1, E)^{\circ} \cup (\tilde{F}_2, E)^{\circ} \subseteq [(\tilde{F}_1, E) \cup (\tilde{F}_2, E)]^{\circ}$.

Proof.

(i) Let $(\tilde{F}_1, E)^{\circ} = (\tilde{F}_2, E)$ Then $(\tilde{F}_2, E) \in \tau iff (\tilde{F}_2, E) = (\tilde{F}_2, E)^{\circ}$. So $[(\tilde{F}_1, E)^{\circ}]^{\circ} = (\tilde{F}_1, E)^{\circ}$.

(ii) Since $0_{(X,E)}$ and $1_{(X,E)}$ are always CSVNS open sets, we have:

$$(0_{(X,E)})^{\circ} = 0_{(X,E)}, \quad \text{and} \quad (1_{(X,E)})^{\circ} = 1_{(X,E)}.$$

(iii) It is known that $(\tilde{F}_1, E)^{\circ} \subseteq (\tilde{F}_1, E) \subseteq (\tilde{F}_2, E)$ and $(\tilde{F}_2, E)^{\circ} \subseteq (\tilde{F}_2, E)$. Since $(\tilde{F}_2, E)^{\circ}$ is the biggest complex single-valued neutrosophic soft open set contained in $(\tilde{F}_2, E)$ and so $(\tilde{F}_1, E)^{\circ} \subseteq (\tilde{F}_2, E)^{\circ}$.

(iv) Since $(\tilde{F}_1, E) \cap (\tilde{F}_2, E) \subseteq (\tilde{F}_1, E)$ and $(\tilde{F}_1, E) \cap (\tilde{F}_2, E) \subseteq (\tilde{F}_2, E)$, then $[(\tilde{F}_1, E) \cap (\tilde{F}_2, E)]^{\circ} \subseteq (\tilde{F}_1, E)^{\circ}$ and $[(\tilde{F}_1, E) \cap (\tilde{F}_2, E)]^{\circ} \subseteq (\tilde{F}_2, E)^{\circ}$ and so,

$$[(\tilde{F}_1, E) \cap (\tilde{F}_2, E)]^{\circ} \subseteq (\tilde{F}_1, E)^{\circ} \cap (\tilde{F}_2, E)^{\circ}.$$

On the other hand, since $(\tilde{F}_1, E)^{\circ} \subseteq (\tilde{F}_1, E)$ and $(\tilde{F}_2, E)^{\circ} \subseteq (\tilde{F}_2, E)$, then:

$$(\tilde{F}_1, E)^{\circ} \cap (\tilde{F}_2, E)^{\circ} \subseteq (\tilde{F}_1, E) \cap (\tilde{F}_2, E).$$

Besides,$[(\tilde{F}_1, E) \cap (\tilde{F}_2, E)]^{\circ} \subseteq (\tilde{F}_1, E) \cap (\tilde{F}_2, E)$ and is the biggest complex single-valued neutrosophic soft open set. Therefore, $(\tilde{F}_1, E)^{\circ} \cap (\tilde{F}_2, E)^{\circ} \subseteq [(\tilde{F}_1, E) \cap (\tilde{F}_2, E)]^{\circ}$. Thus, $[(\tilde{F}_1, E) \cap (\tilde{F}_2, E)]^{\circ} = (\tilde{F}_1, E)^{\circ} \cap (\tilde{F}_2, E)^{\circ}$.

(v) Since $(\tilde{F}_1, E) \subseteq (\tilde{F}_1, E) \cup (\tilde{F}_2, E)$ and $(\tilde{F}_2, E) \subseteq (\tilde{F}_1, E) \cup (\tilde{F}_2, E)$, then:

$$(\tilde{F}_1, E)^{\circ} \subseteq [(\tilde{F}_1, E) \cup (\tilde{F}_2, E)]^{\circ}, \quad \text{and} \quad (\tilde{F}_2, E)^{\circ} \subseteq [(\tilde{F}_1, E) \cup (\tilde{F}_2, E)]^{\circ}.$$

Therefore,

$$(\tilde{F}_1, E)^{\circ} \cup (\tilde{F}_2, E)^{\circ} \subseteq [(\tilde{F}_1, E) \cup (\tilde{F}_2, E)]^{\circ}.$$

Definition 18. *Let (X,τ,E) be a complex single-valued neutrosophic soft topological space over X and $(\tilde{F},E)\in CSVNSS(X,E)$ be a CSVNSS. Then, the complex single-valued neutrosophic soft closure of $(\tilde{F},E)$, denoted by $\overline{(\tilde{F},E)}$ is defined as the complex single-valued neutrosophic soft intersection of all the complex single-valued neutrosophic soft closed supersets of $(\tilde{F},E)$. Clearly $\overline{(\tilde{F},E)}$ is smallest complex single-valued neutrosophic soft closed set that is containing $(\tilde{F},E)$.*

Example 6. *Let us consider the complex single-valued neutrosophic soft topology τ_1 given in Example 2.Suppose that an any $(\tilde{F},E)\in CSVNSS(X,E)$ is defined as following:*

$$(\tilde{F},E)=\begin{bmatrix} e_1=\langle x_1,0.2e^{\iota\pi(0.1)},0.3e^{\iota\pi(0.2)},0.9e^{\iota\pi(0.8)}\rangle,\langle x_2,0.5e^{\iota\pi(0.4)},0.2e^{\iota\pi(0.1)},0.8e^{\iota\pi(0.8)}\rangle \\ \quad \langle x_3,0.2e^{\iota\pi(0.1)},0.2e^{\iota\pi(0.1)},0.7e^{\iota\pi(0.9)}\rangle; \\ e_2=\langle x_1,0.1e^{\iota\pi(0.1)},0.2e^{\iota\pi(0.1)},0.8e^{\iota\pi(0.9)}\rangle,\langle x_2,0.1e^{\iota\pi(0.1)},0.2e^{\iota\pi(0.1)},0.9e^{\iota\pi(0.8)}\rangle, \\ \quad \langle x_3,0.4e^{\iota\pi(0.3)},0.2e^{\iota\pi(0.1)},0.9e^{\iota\pi(0.9)}\rangle. \end{bmatrix}$$

Obviously, $(0_{(X,E)})^c,(1_{(X,E)})^c,(\tilde{F}_1,E)^c,(\tilde{F}_2,E)^c,and(\tilde{F}_3,E)^c$ are all complex single-valued neutrosophic soft closed sets over (X,τ_1,E). They are given as following:

$$(0_{(X,E)})^c=1_{(X,E)},\quad (1_{(X,E)})^c=0_{(X,E)}$$

$$(\tilde{F}_1,E)^c=\begin{bmatrix} e_1=\langle x_1,0.9e^{\iota\pi(0.9)},0.4e^{\iota\pi(0.2)},0.3e^{\iota\pi(0.5)}\rangle,\langle x_2,0.7e^{\iota\pi(0.7)},0.4e^{\iota\pi(0.5)},0.5e^{\iota\pi(0.4)}\rangle \\ \quad \langle x_3,0.4e^{\iota\pi(0.3)},0.5e^{\iota\pi(0.8)},0.4e^{\iota\pi(0.2)}\rangle; \\ e_2=\langle x_1,0.7e^{\iota\pi(0.9)},0.7e^{\iota\pi(0.2)},0.4e^{\iota\pi(0.7)}\rangle,\langle x_2,0.6e^{\iota\pi(0.5)},0.5e^{\iota\pi(0.3)},0.4e^{\iota\pi(0.2)}\rangle, \\ \quad \langle x_3,0.7e^{\iota\pi(0.8)},0.6e^{\iota\pi(0.6)},0.3e^{\iota\pi(0.4)}\rangle. \end{bmatrix}$$

$$(\tilde{F}_2,E)^c=\begin{bmatrix} e_1=\langle x_1,0.7e^{\iota\pi(0.8)},0.5e^{\iota\pi(0.6)},0.5e^{\iota\pi(0.5)}\rangle,\langle x_2,0.6e^{\iota\pi(0.4)},0.5e^{\iota\pi(0.5)},0.7e^{\iota\pi(0.6)}\rangle \\ \quad \langle x_3,0.3e^{\iota\pi(0.2)},0.6e^{\iota\pi(0.8)},0.6e^{\iota\pi(0.8)}\rangle; \\ e_2=\langle x_1,0.6e^{\iota\pi(0.6)},0.8e^{\iota\pi(0.4)},0.5e^{\iota\pi(0.7)}\rangle,\langle x_2,0.5e^{\iota\pi(0.4)},0.6e^{\iota\pi(0.9)},0.6e^{\iota\pi(0.7)}\rangle, \\ \quad \langle x_3,0.4e^{\iota\pi(0.3)},0.7e^{\iota\pi(0.7)},0.5e^{\iota\pi(0.4)}\rangle. \end{bmatrix}$$

$$(\tilde{F}_3,E)^c=\begin{bmatrix} e_1=\langle x_1,0.5e^{\iota\pi(0.6)},0.6e^{\iota\pi(0.8)},0.6e^{\iota\pi(0.5)}\rangle,\langle x_2,0.4e^{\iota\pi(0.2)},0.7e^{\iota\pi(0.9)},0.7e^{\iota\pi(0.7)}\rangle \\ \quad \langle x_3,0.2e^{\iota\pi(0.1)},0.7e^{\iota\pi(0.8)},0.8e^{\iota\pi(0.9)}\rangle; \\ e_2=\langle x_1,0.4e^{\iota\pi(0.3)},0.8e^{\iota\pi(0.9)},0.6e^{\iota\pi(0.8)}\rangle,\langle x_2,0.4e^{\iota\pi(0.3)},0.8e^{\iota\pi(0.9)},0.8e^{\iota\pi(0.9)}\rangle, \\ \quad \langle x_3,0.3e^{\iota\pi(0.2)},0.7e^{\iota\pi(0.9)},0.6e^{\iota\pi(0.5)}\rangle. \end{bmatrix}$$

Then $(1_{(X,E)})^c,(\tilde{F}_1,E)^c,(\tilde{F}_2,E)^c,(\tilde{F}_3,E)^c\supseteq(\tilde{F},E)$. Therefore,

$$\overline{(\tilde{F},E)}=(1_{(X,E)})^c\cap(\tilde{F}_1,E)^c\cap(\tilde{F}_3,E)^c\cap(\tilde{F}_2,E)^c=(\tilde{F}_3,E)^c$$

.

Theorem 3. *Let (X,τ,E) be a complex single-valued neutrosophic soft topological space over X and $(\tilde{F},E)\in CSVNSS(X,E)$. $(\tilde{F},E)$ is a complex single-valued neutrosophic soft closed set and iff $(\tilde{F},E)=\overline{(\tilde{F},E)}$*

Proof. Let $(\tilde{F},E)$ be a complex single-valued neutrosophic soft closed set. Then the smallest complex single-valued neutrosophic soft open set that containing $(\tilde{F},E)$ is equal to $(\tilde{F},E)$. Hence, $(\tilde{F},E)=\overline{(\tilde{F},E)}$

Conversely, it is known that $\overline{(\tilde{F},E)}$ is a complex single-valued neutrosophic soft closed set and if $(\tilde{F},E)=\overline{(\tilde{F},E)}$, then $(\tilde{F},E)$ is a complex single-valued neutrosophic soft closed set.

Theorem 4. *Let (X, τ, E) be a complex single-valued neutrosophic soft topological space over X and $(\tilde{F}_1, E), (\tilde{F}_2, E) \in CSVNSS(X, E)$. Then,*

(i) $\overline{\overline{[(\tilde{F}, E)]}} = \overline{(\tilde{F}, E)}$,

(ii) $\overline{(0_{(X,E)})} = 0_{(X,E)}$ *and* $\overline{(1_{(X,E)})} = 1_{(X,E)}$,

(iii) $(\tilde{F}_1, E) \subseteq (\tilde{F}_2, E) \Rightarrow \overline{(\tilde{F}_1, E)} \subseteq \overline{(\tilde{F}_2, E)}$,

(iv) $\overline{[(\tilde{F}_1, E) \cup (\tilde{F}_2, E)]} = \overline{(\tilde{F}_1, E)} \cup \overline{(\tilde{F}_2, E)}$,

(v) $\overline{(\tilde{F}_1, E)} \cap \overline{(\tilde{F}_2, E)} \subseteq \overline{[(\tilde{F}_1, E) \cap (\tilde{F}_2, E)]}$.

Proof.

(i) Let $\overline{(\tilde{F}_1, E)} = (\tilde{F}_2, E)$ Then $(\tilde{F}_2, E)$ a complex single-valued neutrosophic soft closed set.Hence $(\tilde{F}_2, E)$ and $\overline{(\tilde{F}_2, E)}$ are equal. Therefore $\overline{\overline{[(\tilde{F}_1, E)]}} = \overline{(\tilde{F}_1, E)}$.

(ii) Since $0_{(X,E)}$ and $1_{(X,E)}$ are always CSVNS closed sets, we have:

$$\overline{(0_{(X,E)})} = 0_{(X,E)}, \quad \text{and} \quad \overline{(1_{(X,E)})} = 1_{(X,E)}.$$

(iii) It is known that $(\tilde{F}_1, E) \subseteq \overline{(\tilde{F}_1, E)}$ and $(\tilde{F}_2, E) \subseteq \overline{(\tilde{F}_2, E)}$, so $(\tilde{F}_1, E) \subseteq (\tilde{F}_2, E) \subseteq \overline{(\tilde{F}_2, E)}$. Since $\overline{(\tilde{F}_2, E)}$ is the smallest complex single-valued neutrosophic soft closed set containing $(\tilde{F}_1, E)$, then $\overline{(\tilde{F}_1, E)} \subseteq \overline{(\tilde{F}_2, E)}$.

(iv) Since $(\tilde{F}_1, E) \subseteq (\tilde{F}_1, E) \cup (\tilde{F}_2, E)$ and $(\tilde{F}_2, E) \subseteq (\tilde{F}_1, E) \cup (\tilde{F}_2, E)$, then $\overline{(\tilde{F}_1, E)} \subseteq \overline{[(\tilde{F}_1, E) \cup (\tilde{F}_2, E)]}$ and $\overline{(\tilde{F}_2, E)} \subseteq \overline{[(\tilde{F}_1, E) \cup (\tilde{F}_2, E)]}$ and so,

$$\overline{(\tilde{F}_1, E)} \cup \overline{(\tilde{F}_2, E)} \subseteq \overline{[(\tilde{F}_1, E) \cup (\tilde{F}_2, E)]}.$$

Conversely, since $(\tilde{F}_1, E) \subseteq \overline{(\tilde{F}_1, E)}$ and $(\tilde{F}_2, E) \subseteq \overline{(\tilde{F}_2, E)}$, then:

$$(\tilde{F}_1, E) \cup (\tilde{F}_2, E) \subseteq \overline{(\tilde{F}_1, E)} \cup \overline{(\tilde{F}_2, E)}.$$

Besides,$\overline{[(\tilde{F}_1, E) \cup (\tilde{F}_2, E)]}$ and is the smallest complex single-valued neutrosophic soft closed set that containing $(\tilde{F}_1, E) \cup (\tilde{F}_2, E)$. Therefore, $\overline{[(\tilde{F}_1, E) \cup (\tilde{F}_2, E)]} \subseteq \overline{(\tilde{F}_1, E)} \cup \overline{(\tilde{F}_2, E)}$. Thus, $\overline{[(\tilde{F}_1, E) \cup (\tilde{F}_2, E)]} = \overline{(\tilde{F}_1, E)} \cup \overline{(\tilde{F}_2, E)}$.

(v) Since

$$(\tilde{F}_1, E) \cap (\tilde{F}_2, E) \subseteq \overline{[(\tilde{F}_1, E) \cap (\tilde{F}_2, E)]}, \quad \text{and} \quad \overline{[(\tilde{F}_1, E) \cap (\tilde{F}_2, E)]}.$$

is the smallest complex single-valued neutrosophic soft closed set that containing $(\tilde{F}_1, E) \cap (\tilde{F}_2, E)$. Then,

$$\overline{[(\tilde{F}_1, E) \cap (\tilde{F}_2, E)]} \subseteq \overline{(\tilde{F}_1, E)} \cap \overline{(\tilde{F}_2, E)}.$$

Theorem 5. *Let (X, τ, E) be a complex single-valued neutrosophic soft topological space over X, and let $(\tilde{F}, E) \in CSVNSS(X, E)$. Then:*

(i) $\overline{[(\tilde{F}, E)]^c} = [(\tilde{F}, E)^c]^\circ$,

(ii) $[(\tilde{F}, E)^\circ]^c = \overline{[(\tilde{F}, E)^c]}$.

Proof.

(i)

$$\begin{aligned}\overline{(\tilde{F},E)} &= \cap\{(\tilde{G},E)\in\tau^c : (\tilde{G},E)\supseteq(\tilde{F},E)\}\\ &\Rightarrow [\overline{(\tilde{F},E)}]^c = \left[\cap\{(\tilde{G},E)\in\tau^c : (\tilde{G},E)\supseteq(\tilde{F},E)\}\right]^c\\ &= \cup\{(\tilde{G},E)^c\in\tau : (\tilde{G},E)^c\subseteq(\tilde{F},E)^c\}\\ &= [(\tilde{F},E)^c]^\circ.\end{aligned}$$

(ii)

$$\begin{aligned}(\tilde{F},E)^\circ &= \cup\{(\tilde{G},E)\in\tau : (\tilde{G},E)\subseteq(\tilde{F},E)\}\\ &\Rightarrow [(\tilde{F},E)^\circ]^c = \left[\cap\{(\tilde{G},E)\in\tau : (\tilde{G},E)\subseteq(\tilde{F},E)\}\right]^c\\ &= \cap\{(\tilde{G},E)^c\in\tau^c : (\tilde{G},E)^c\supseteq(\tilde{F},E)^c\}\\ &= \overline{[(\tilde{F},E)^c]}.\end{aligned}$$

5. Complex Neutrosophic Soft Set-Based Cotangent Similarity Approach for Multi-Source Signal Analysis

One such analytical technique for determining how similar two vectors (data) are is the cotangent similarity measure (CSM). It can be used in a wide range of fields that include machine learning, image processing, and data analysis. CSM will be able to identify differences and dependencies that would have gone unnoticed in the absence of pure distance-based measurements by taking into account the geometric orientation of the data points. It is frequently used in data analysis, machine learning, and image processing. In the event of military operations, CSM can be used to classify potential targets based on the surveillance data. This is accomplished by comparing a target's operational characteristics to those of known classified profiles. The likelihood that the threats will be compared and classed appropriately is then increased by estimating the degree to which a target fits into pre-existing categories of threats. The classification and pattern recognition tasks are aided by a collection of machine learning and visualization methods. Sig: Pearson Correlation, Elbow Method, Spline Interpolation, PCA, K-Means, K-Means++, and t-SNE.

5.1. Cotangent similarity measures

Let $T_i = (T_{ik}, I_{ik}, F_{ik}), C_j = (T_{jk}, I_{jk}, F_{jk})$ are two CNSSs. Each set is represented by three components for each feature k:
T_{ik}: Truth-membership of feature $kforT_i$.
I_{ik}: Indeterminacy-membership of feature $kforT_i$.
F_{ik}: Falsity-membership degree of feature $kforT_i$.
The values typically satisfy: $T_{ik}, I_{ik}, F_{ik} \in [0,1]$
Similarly, for object C_j:
T_{jk}: Truth-membership of feature $kforC_j$.
I_{jk}: Indeterminacy-membership of feature $kforC_j$.
F_{jk}: Falsity-membership degree of feature $kforC_j$.
The values typically satisfy: $T_{jk}, I_{jk}, F_{jk} \in [0,1]$.

The cotangent similarity measures between T_i and C_j is defined as:
$Cotangent_{SCNSS}(T_i, C_j) =$

$$\frac{1}{n}\sum_{k=1}^{n}\{\cot[\frac{\pi}{4}+\frac{\pi}{12}(|T_{ik}-T_{jk}|+|I_{ik}-I_{jk}|+|F_{ik}-F_{jk}|)]\}$$

5.2. Real-time military target classification with cotangent similarity and advanced surveillance data integration

Using the multi-source signal samples $S = \{S_1, S_2, S_3\}$ to accurately categorize the operational targets $T = \{T_1, T_2, T_3\}$ and then applying them to the appropriate operational classes $C = \{C_1, C_2, C_3\}$ is the primary task in the current surveillance and reconnaissance systems. The available information on each target is inherently ambiguous, imprecise, and diverse; it includes heat emissions, radar signatures, electronic monitoring, and other signal measures. This uncertainty necessitates a mathematical procedure that can simultaneously handle truth, indeterminacy, and falsity. The relationship between targets, signals, and classes in a multifaceted environment is related in terms of event-based measures (e) and their corresponding measures in the operational classification table (Table 2). However, overlapping values, inconsistent reliability, and nonlinear relationships between features make it impossible to directly compare a response of raw signals between targets and classes. This is resolved by proposing a Cotangent similarity measure based on the complex neutrosophic soft set (Cotangent CNSS) framework, which enables the measurement of each target-class pair's similarity. It considers the joint contribution of the truth-membership, indeterminacy-membership, and falsity-membership functions, normalized with respect to $n = 3$ attributes, in each pair (T_i, C_j). Cotangent similarity scores are generated as a result, and these can be used to rank candidate target profiles in relation to operational class templates.

Table 1: Matrix of Target Intelligence Features Based on Cotangent Similarity ($T \times S$)

	S_1	S_2	...	S_n
T_1	T_{11}, I_{11}, F_{11}	T_{12}, I_{12}, F_{12}	...	T_{1n}, I_{1n}, F_{1n}
T_2	T_{21}, I_{21}, F_{21}	T_{22}, I_{22}, F_{22}	...	T_{2n}, I_{2n}, F_{2n}
...	...	...	...	...
T_m	T_{m1}, I_{m1}, F_{m1}	T_{m2}, I_{m2}, F_{m2}	...	T_{mn}, I_{mn}, F_{mn}

The raw surveillance parameters for each target T_i, as gathered from each data source S_i, are displayed in this table 1. These are represented by the 3-dimensional feature vectors found in each cell, gives each target-source combination a thorough feature profile for preliminary analysis and threat modeling.

Table 2: Operational Classification Matrix for Target Surveillance Data ($T \times S \to C$)

Row-I	S_1	S_2	S_3	**Row-II**	C_1	C_2	C_3
T_1	$\begin{pmatrix} 0.5e^{\iota\pi(0.6)} \\ 0.7e^{\iota\pi(0.5)} \\ 0.3e^{\iota\pi(0.3)} \end{pmatrix}$	$\begin{pmatrix} 0.6e^{\iota\pi(0.7)} \\ 0.4e^{\iota\pi(0.4)} \\ 0.3e^{\iota\pi(0.4)} \end{pmatrix}$	$\begin{pmatrix} 0.3e^{\iota\pi(0.2)} \\ 0.5e^{\iota\pi(0.5)} \\ 0.8e^{\iota\pi(0.3)} \end{pmatrix}$	S_1	$\begin{pmatrix} 0.3e^{\iota\pi(0.4)} \\ 0.5e^{\iota\pi(0.7)} \\ 0.7e^{\iota\pi(0.7)} \end{pmatrix}$	$\begin{pmatrix} 0.7e^{\iota\pi(0.6)} \\ 0.6e^{\iota\pi(0.5)} \\ 0.2e^{\iota\pi(0.3)} \end{pmatrix}$	$\begin{pmatrix} 0.5e^{\iota\pi(0.8)} \\ 0.4e^{\iota\pi(0.7)} \\ 0.9e^{\iota\pi(0.3)} \end{pmatrix}$
T_2	$\begin{pmatrix} 0.4e^{\iota\pi(0.6)} \\ 0.7e^{\iota\pi(0.9)} \\ 0.5e^{\iota\pi(0.7)} \end{pmatrix}$	$\begin{pmatrix} 0.2e^{\iota\pi(0.4)} \\ 0.4e^{\iota\pi(0.9)} \\ 0.6e^{\iota\pi(0.3)} \end{pmatrix}$	$\begin{pmatrix} 0.7e^{\iota\pi(0.7)} \\ 0.4e^{\iota\pi(0.3)} \\ 0.6e^{\iota\pi(0.6)} \end{pmatrix}$	S_2	$\begin{pmatrix} 0.2e^{\iota\pi(0.5)} \\ 0.3e^{\iota\pi(0.2)} \\ 0.7e^{\iota\pi(0.3)} \end{pmatrix}$	$\begin{pmatrix} 0.6e^{\iota\pi(0.6)} \\ 0.7e^{\iota\pi(0.8)} \\ 0.4e^{\iota\pi(0.3)} \end{pmatrix}$	$\begin{pmatrix} 0.3e^{\iota\pi(0.6)} \\ 0.6e^{\iota\pi(0.7)} \\ 0.8e^{\iota\pi(0.9)} \end{pmatrix}$
T_3	$\begin{pmatrix} 0.7e^{\iota\pi(0.9)} \\ 0.6e^{\iota\pi(0.5)} \\ 0.8e^{\iota\pi(0.8)} \end{pmatrix}$	$\begin{pmatrix} 0.2e^{\iota\pi(0.4)} \\ 0.8e^{\iota\pi(0.5)} \\ 0.7e^{\iota\pi(0.6)} \end{pmatrix}$	$\begin{pmatrix} 0.6e^{\iota\pi(0.9)} \\ 0.3e^{\iota\pi(0.6)} \\ 0.2e^{\iota\pi(0.3)} \end{pmatrix}$	S_3	$\begin{pmatrix} 0.4e^{\iota\pi(0.4)} \\ 0.7e^{\iota\pi(0.5)} \\ 0.5e^{\iota\pi(0.9)} \end{pmatrix}$	$\begin{pmatrix} 0.6e^{\iota\pi(0.2)} \\ 0.3e^{\iota\pi(0.5)} \\ 0.4e^{\iota\pi(0.4)} \end{pmatrix}$	$\begin{pmatrix} 0.7e^{\iota\pi(0.2)} \\ 0.3e^{\iota\pi(0.8)} \\ 0.2e^{\iota\pi(0.3)} \end{pmatrix}$

This table 2 delineates the cotangent similarity values calculated by comparing the feature vectors of targets with those of established classified operational profiles (e.g., C_1: high-value asset, C_2: decoy, C_3: communication node). The raw cosine similarity between each target (T) and its corresponding surveillance data (S) is presented in Row-I ($T \times S$). Meanwhile, the cotangent similarity between each data source vector and the classified operational profiles is displayed in Row-II ($S \times C$). This method facilitates the prioritization of actions (e.g., attack, monitor, ignore) by classifying or clustering targets according to their correlation with well-defined threat or operational categories.
All target-classification pairings are then averaged by adding the cotangent values that were determined for each pair of targets and categorized profiles.
The values of the resulting cotangent similarities are:
$Cotangent_{SCNSS}(T_1, C_1) = 0.4913$
$Cotangent_{SCNSS}(T_1, C_2) = 0.6653$
$Cotangent_{SCNSS}(T_1, C_3) = 0.5785$
$Cotangent_{SCNSS}(T_2, C_1) = 0.5287$
$Cotangent_{SCNSS}(T_2, C_2) = 0.4937$
$Cotangent_{SCNSS}(T_2, C_3) = 0.3576$
$Cotangent_{SCNSS}(T_3, C_1) = 0.4110$
$Cotangent_{SCNSS}(T_3, C_2) = 0.4604$
$Cotangent_{SCNSS}(T_3, C_3) = 0.4221$

Table 3: Cotangent Similarity scores between signal samples ($S_1 - S_3$) and class templates ($T_1 - T_3$)

Cot SM	S_1	S_2	S_3
T_1	0.4913	0.6653	0.5785
T_2	0.5287	0.4937	0.3576
T_3	0.4110	0.4604	0.4221

The degree to which each signal sample resembles the three class templates is shown in the cotangent similarity table 3. The template is most similar to S_1, although the score is average in the case of S_1, where the maximum similarity with T_2 is 0.5287. The highest match in S_2 with T_1 is 0.6653, which is also the highest value in the entire table. This indicates that S_2 is classified under template T_1 in a strong and reliable manner. The alignment with T_1 in S_3 has the highest similarity, at 0.5785, which falls within a moderate range and is not as definitive as S_2. Overall, the results show that T_1 is capable of drawing in two signals, S_2 and S_3, indicating

that this template is a main or special active profile. Only S_1 is connected to T_2, and their connection is not very strong. T_3 may be utilized as a weak or background category because it does not appear to be the best match to any signal and all of its scores are below the best ones. While S_1T_2 and S_3T_1 require closer interpretation or further investigation, S_2T_1 may be regarded as a specific classification in a realistic option.

6. Result and Discussion

Targets T_1 and T_3's similarity associations are projected onto two principal components (PC1 = 0.65, PC2 = 0.35), whose variability is fully captured in two dimensions, in the PCA clustering plot shown in Fig. 1. The targets are positioned according to how well they align with the centroid clusters of the groups, C_1 and C_2. It reaches Cluster C_2's location on PC1's far right, indicating great stability and centrality in the data structure, in the instance of T_1. This suggests that T_1 is the most appropriate and representative aim. In contrast to both clusters, the point for T_2 is located higher along PC2. It is more of an outlier than a member of the cluster because of its high and unique status, which indicates unique behavior.The point in T_3 is located on the bottom-left, but both PC1 and PC2 have scaled it out. Given that its alignment with T_1 and T_2 is weaker and more divergent, it is distantly related to Cluster C_1. In conclusion, T_1, which is securely attached to Cluster C_1, is the strongest target and the most stable one. T_3 is the weakest, closely matching Cluster C_1, whereas T_2 is independent and detached, exhibiting distinct but less coherent behavior.

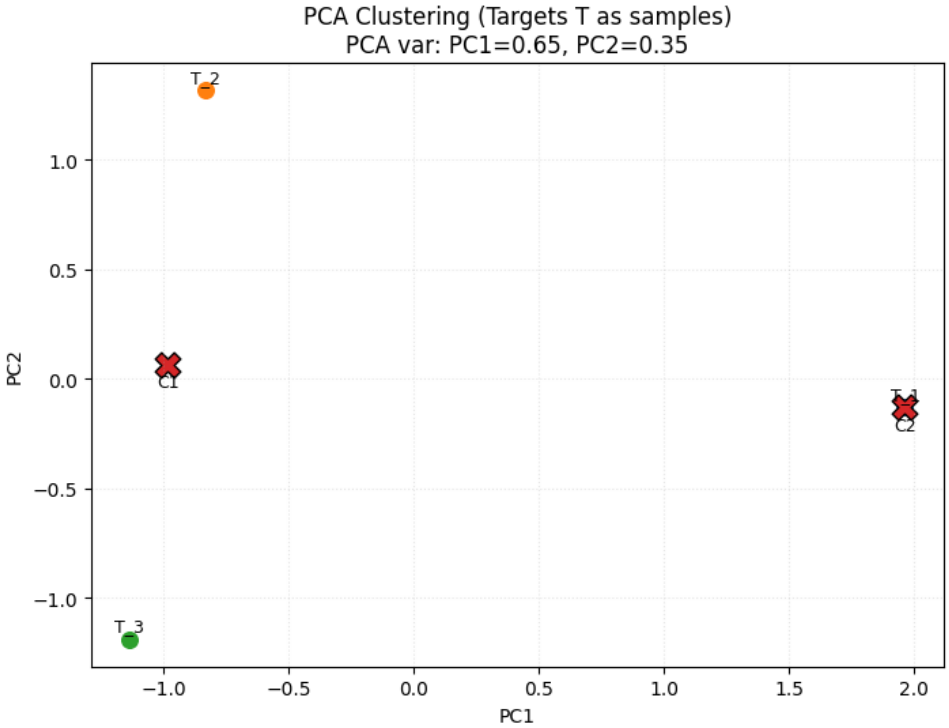

Figure 1

Even though the drawing is shown in three dimensions, Fig. 2 shows that PC1 (65%), PC2 (35%), and PC3 do not contribute to the variance, suggesting that the structure is essentially two-dimensional. The centroid is located near the two apparent clusters that are formed from the points: Cluster 1 on the left and Cluster 2 on the right. The light blue point is more of an outlier or transitional point because it is higher along PC2 rather than between the centroids. Because it is the most central and constant profile, the Cluster 2 point (the right side) is understood as a target and is hence the most representative. The point on the left is more divergent,

indicating less resemblance, whereas the higher light blue point is linked to less cohesive and united conduct. The clustering generally points to a hierarchy where a target is the reference, an outlier is an outlier, and a diverging instance is the last one.

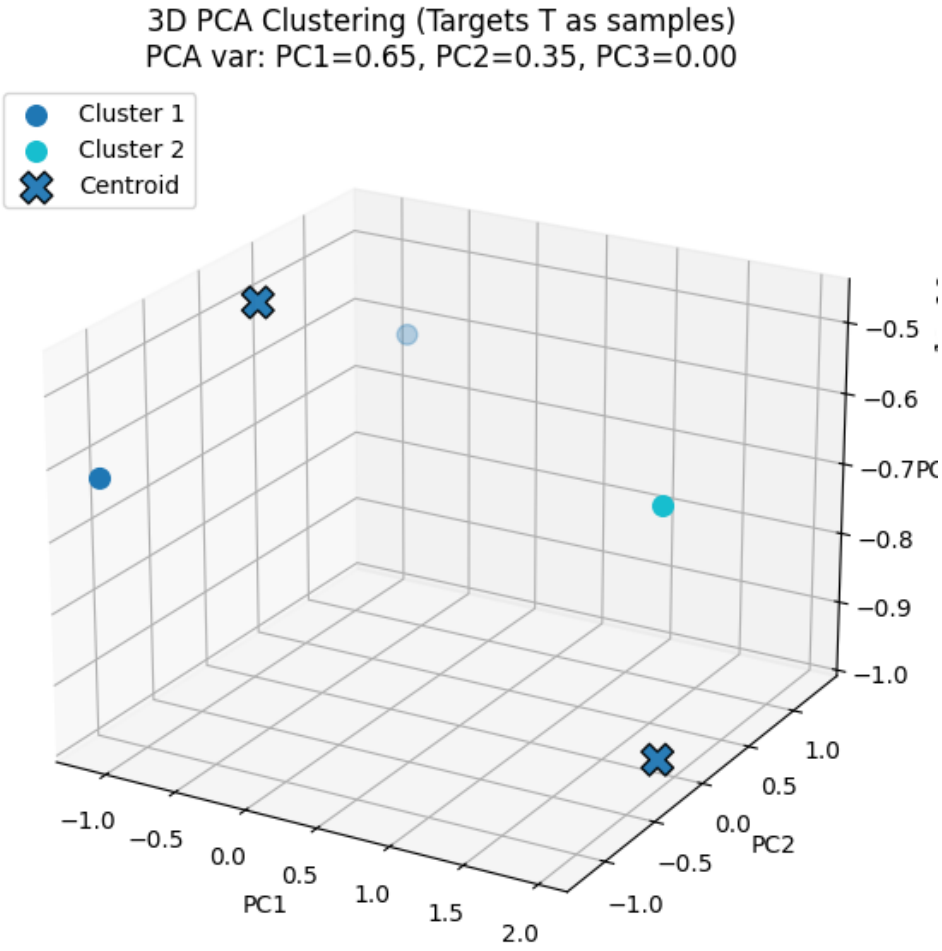

Figure 2

Since this would divide the three targets $(T_1, T_2, T-3)$, the K-Means plot (Fig. 3) employs k = 2 on the Cot SM data. The color coding indicates cluster membership, while the x-axis (S_1) and y-axis (S_2) represent signal similarity coordinates. When it comes to T_1, the point at the top where $S_2 = 0.67$ is clearly separated and is categorized as belonging to Cluster 1 (yellow). It is the strongest and most distinct target in the dataset since it ranks 1 in terms of similarity. T_2's point, which is comparable to Cluster 0 (purple), is on the right where $S_1 = 0.53$ and $S_2 = 0.49$. While not quite enough to match the dominant T_1 cluster, this indicates a moderate level of resemblance. In the example of T_3, Cluster 0 (purple), $S_1 = 0.41$, $S_2 = 0.47$, and the point is at the lower left. As a result, T_3 is the poorest aligned target overall and exhibits weak similarity. All things considered, T_1 forms its high-similarity cluster, highlighting its superiority and distinction from the others. Lower and more similar degrees of similarity are indicated by the T_2 and T_3 clustering towards one another. This demonstrates that T_1 has the greatest influence, while T_2 and T_3 have a weaker, secondary link.

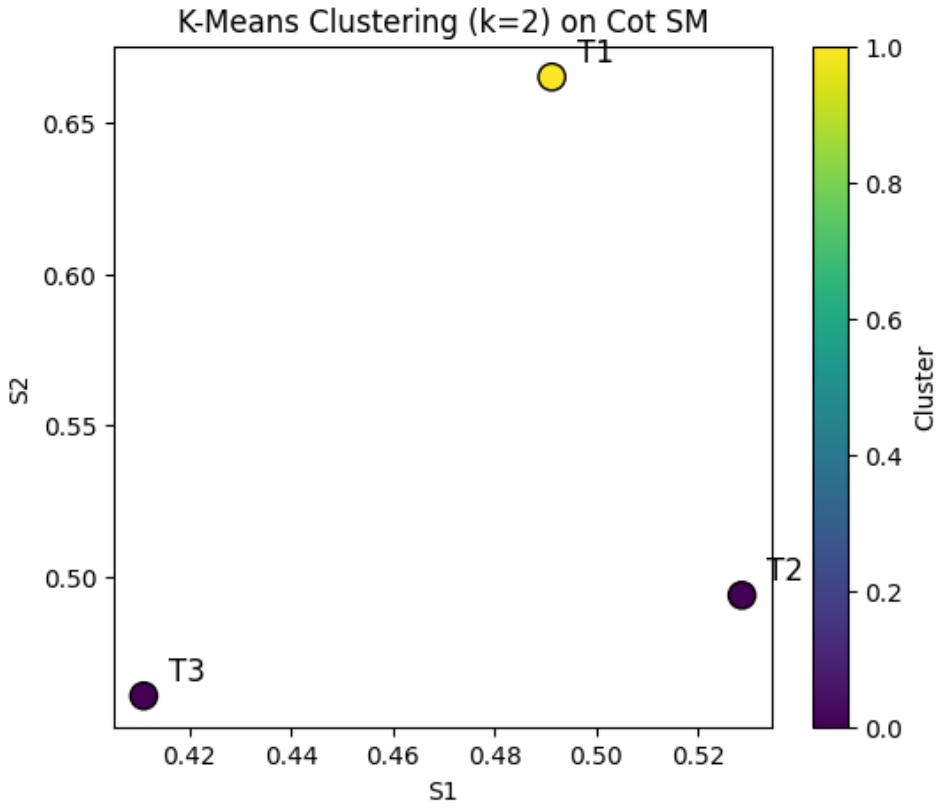

Figure 3

The top three maximum similarities are displayed in Fig. 4's K-Means++ clustering plot. Cluster assignments are coloured, and maxima are circled in red to improve emphasis. Cluster centers are indicated by red X markings. The global maximum level of 0.665 is indicated by the double circle that marks the location on the far right in the instance of T_1 (T_1, S_2). This demonstrates that $T1$, which is clearly distinguished from the others, is the most powerful and dominant target. Instead of being in the cluster's centroid, the point in T3 will be in the lower-left quadrant. It is one of the weakest targets, and its inferior position attests to a slight resemblance. The circled maximum in the yellow location (highlighted on the upper left) indicates another data value with the best performance, but it is still less than the T_1S_2 maximum. Although it does not win out globally, this contributes to the cluster balance. T_1 is the most potent target, producing the worldwide maximum (0.665) and focusing intently on its centroid, to sum up. Other emphasized maxima show supplementary substantial contributions that do not dominate T_1, and T_3 is the weakest and not connected to dominant regions.

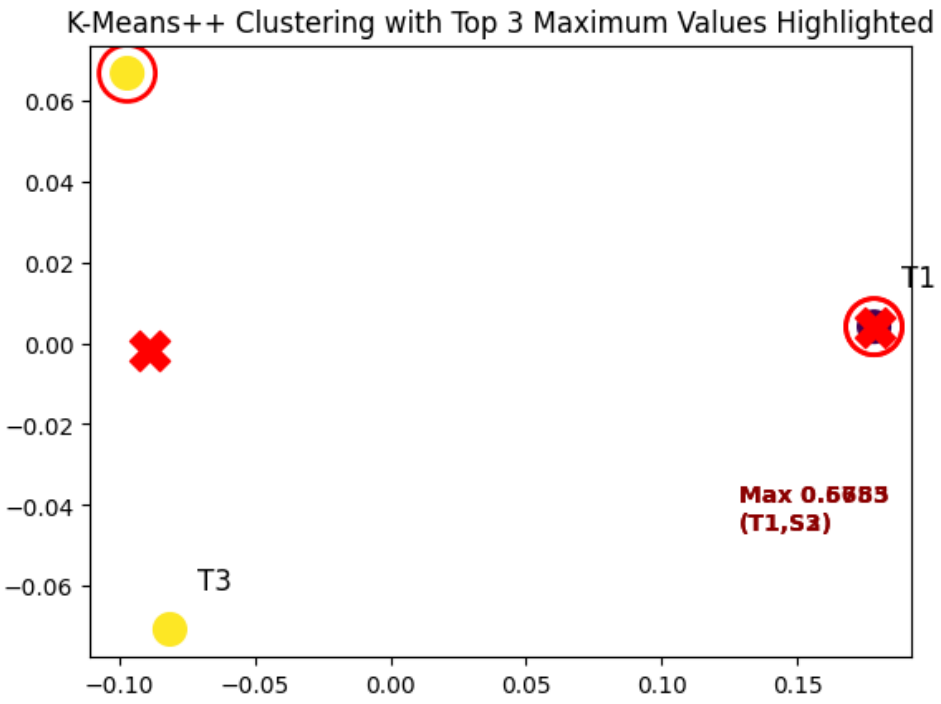

Figure 4

A reduction of the PCA applied to the Iris data set is used in the K-Means clustering plot (Fig. 5), where the data is shown on the two main components. Red X markers, which show the cluster centers, are used to color the individual samples according to the cluster to which they belong. Each sample counts as one point. The samples are highly concentrated when PC1 is negative in the case of the left clustered (teal points). With low levels of within-cluster variance and high levels of cohesiveness, the centroid is located in the center of the cluster. This indicates a grouping that is precise and unambiguous. In PC1 and PC2, the middle cluster samples (purple spots) are dispersed more widely. The dispersion suggests that there is less cohesion than with the teal cluster, even if the centroid is near the geometrical center. This suggests that this group is more internally variable. The samples in the most right cluster (yellow points) are moderately dispersed in PC2 and broadly dispersed in PC1's positive values. In order to balance the wider range of data points, the centroid is likewise positioned near the center of mass. The cluster stands apart from the other two, although selling more broadly. In summary, the yellow cluster is bigger but clearly split, the purple cluster is somewhat cohesive but more variable, and the teal cluster is the smallest and tightest. The centroids' positions provide for successful separation within the three clusters following PCA reduction.

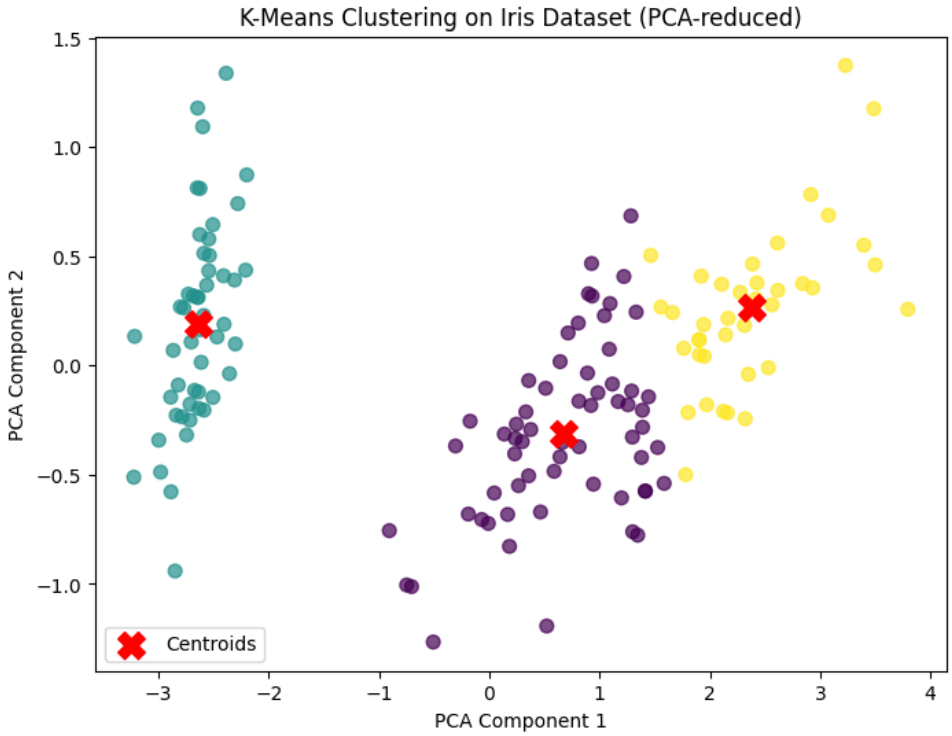

Figure 5

The K-Means clustering graphic in Fig. 6 maps the samples onto two main components for visualization and applies PCA reduction to the normalized Iris datasets. With its unique cluster colors and red markers of X that represent the computed centroid, each point represents a single sample. The samples are concentrated along the negative PC1 and PC2 in the case of the left cluster (teal points). The centroid has a tight structure, a high degree of cohesion, and is near the geometric center. The fact that this cluster is the most compact suggests that there is little variation within it. Samples in the middle section of the PC1 and PC2 are widely dispersed in the case of the middle cluster (purple points). In comparison to the teal cluster, the centroid is at the center, and the dispersion is larger, suggesting less cohesion. The members in this category are more diverse. The right cluster (yellow dots) contains samples that are modest in PC2 and broad in positive PC1 values. Despite having a wider spread, the centroid centers the cluster by balancing this distribution. Though not as compact as the teal cluster, this cluster is clearly unique from the others. The yellow cluster is wide and well-separated, suggesting good partitioning of the normalized data set after PCA reduction, the purple cluster is bigger and of moderate cohesion, and the teal cluster is the most compact and internally consistent cluster overall.

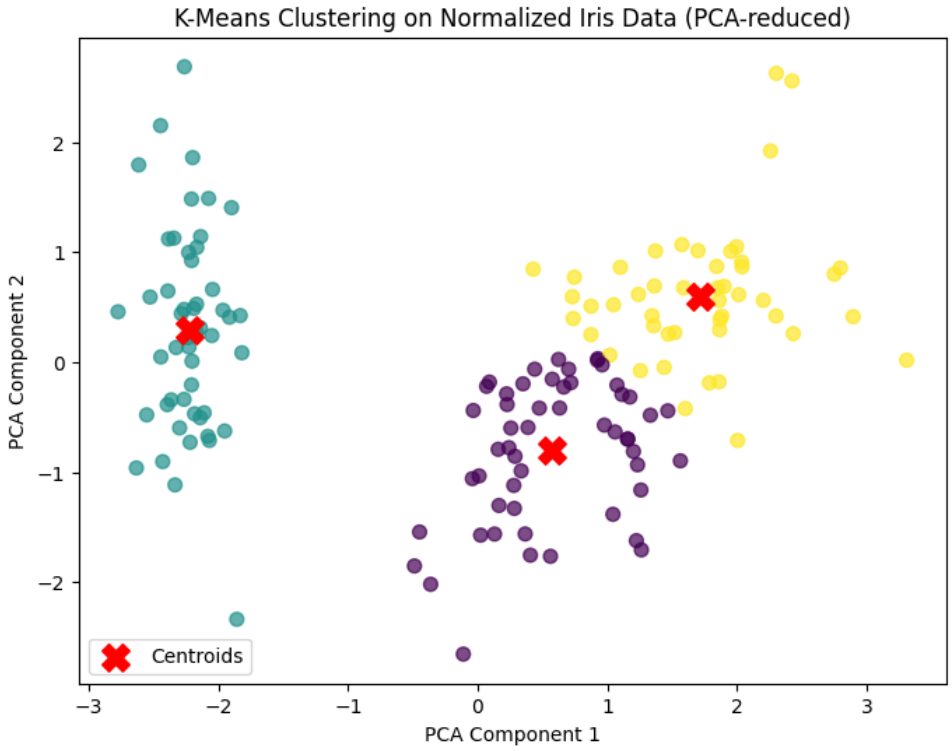

Figure 6

A line represents a sample, and the colors represent the species setosa (red), versicolor (green), and virginica (blue) in the 3D t-SNE representation of the Iris data in parallel coordinates shown in Fig. 7. The three dimensions of t-SNE are represented by these axes, and the line patterns show how samples of each class are projected onto the reduced features space. In the case of setosa (red lines), the values in the lower portions of the dimensions are aggregated, and the cluster is clearly identified. The general downward inclination of t-SNE1 and t-SNE2 is noteworthy and illustrates the species' high degree of coherence and distinctiveness. Versicolor (green lines) has more interlacing paths. They overlap with both setosa and virginica and occupy an intermediate position in all dimensions. Versicolor is more intermediate in the structure of the Iris dataset since it is less segregated. Particularly along t-SNE1 and t-SNE3, the values are nearer bigger values in the case of virginica (blue lines). In addition to being more regular than the green, the blue lines exhibit a reasonably compact grouping, despite some versicolor overlap. The traditional structure of the Iris data set is demonstrated by the t-SNE parallel coordinates, which show that the most distinct and well-separated species, setosa, is at the center with versicolor and virginica, which are rather compact and partially overlap with the former, indicating the boundary between the two.

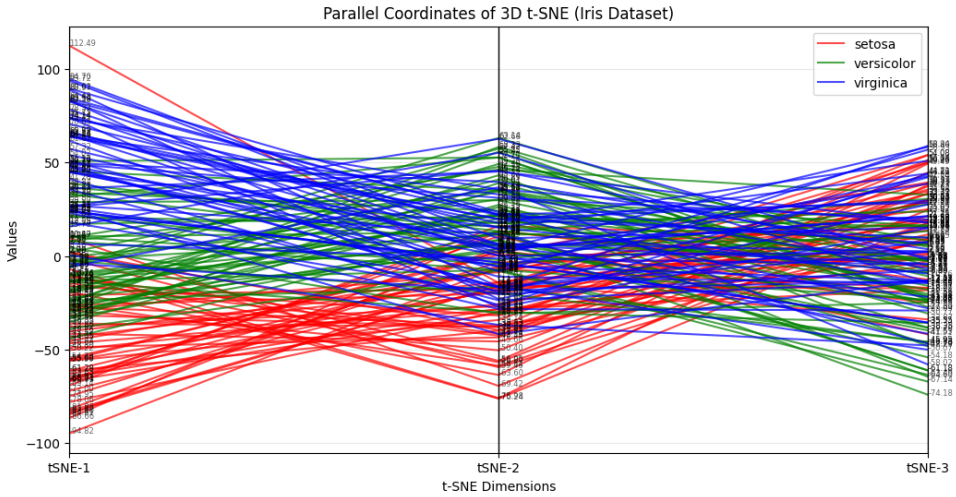

Figure 7

The tie between $\grave{X}$ and Y is depicted in Fig. 8, where the bluish line represents the spline interpolation and the red dots represent the initial data points. The noise in the raw data is removed, and the curve emphasizes local variances. The curve climbs through the mid-range X values to a local maximum at zero after beginning at a moderate value of Y 0.26 at low $\grave{X}$, reaching an early high at 0.73, and a local minimum at -0.54. After this drop, the functional steadily recovers and moves back into the positive area. The green-marked locations of $X = 8$ and $Y = 0.83$ represent the world's maximum point. Higher than the first two peaks, this is the spline's maximum alignment to the data. Other noteworthy positive numbers, such as 0.59 and 0.61, are also noted, but they fall short of the final highlighted maximum. In summary, the spline-smoothed curve exhibits a cyclic wave-like tendency with alternating peaks and troughs. The dominant maximum (0.83) supports the strongest functional reaction, whereas the successive increases and declines are the intermediate changes that surround the main trend.

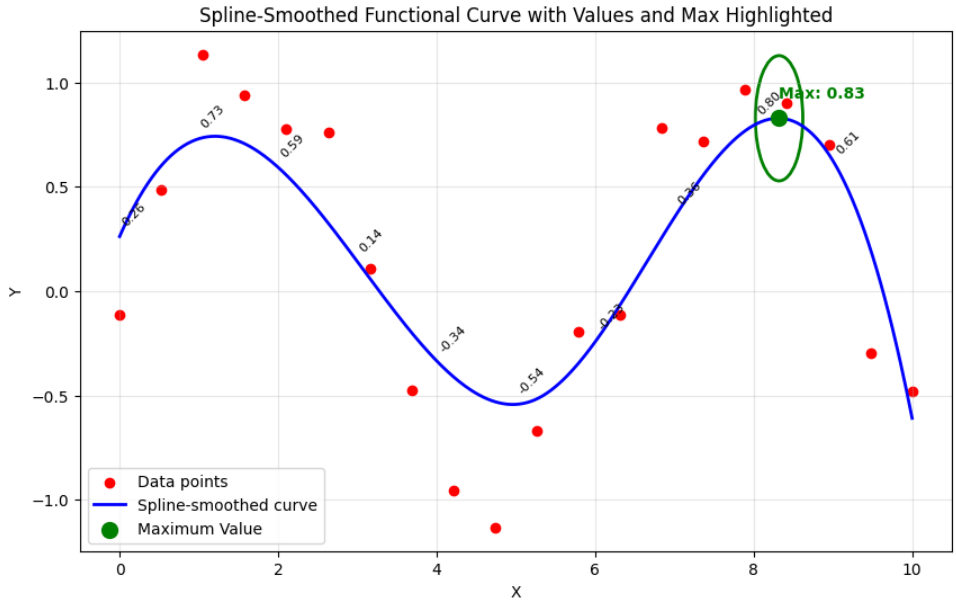

Figure 8

With normal axes of S_1 and S_2, Fig. 9 employs a K-Means clustering normalized plot with $k = 2$ on the Cot SM values. With the scale displayed on the right, the targets $(T_1 - T_3)$ are

on normalized coordinates, and the color designates the clusters. T_1 is assigned to Cluster 1 (yellow), and the point is located in the upper-right corner ($S_1 = 1.0, \quad S_2 = 1.0$). T_1 is the strongest and most common target, as evidenced by the fact that it is at the extreme and lies at maximum normalized values. Similar to Cluster 0 (dark blue), the point in T_2 is on the far right and in the lower region ($S_1 = 0.1, \quad S_2 = 0.17$). This indicates partial but uneven strength due to high performance in S_1 and poor fit in S_2.Cluster 0 (dark blue) is also responsible for the point in T_3, which is located at the bottom-left ($S_1 = 0.0, \quad S_2 = 0.0$). T_3's low normalized values confirm that it is the weakest and least aligned target. T_1 is the most powerful target, forming its own high-value cluster. T_2 and T_3 are grouped in the weaker cluster, with T_2's contribution being somewhat greater than T's.

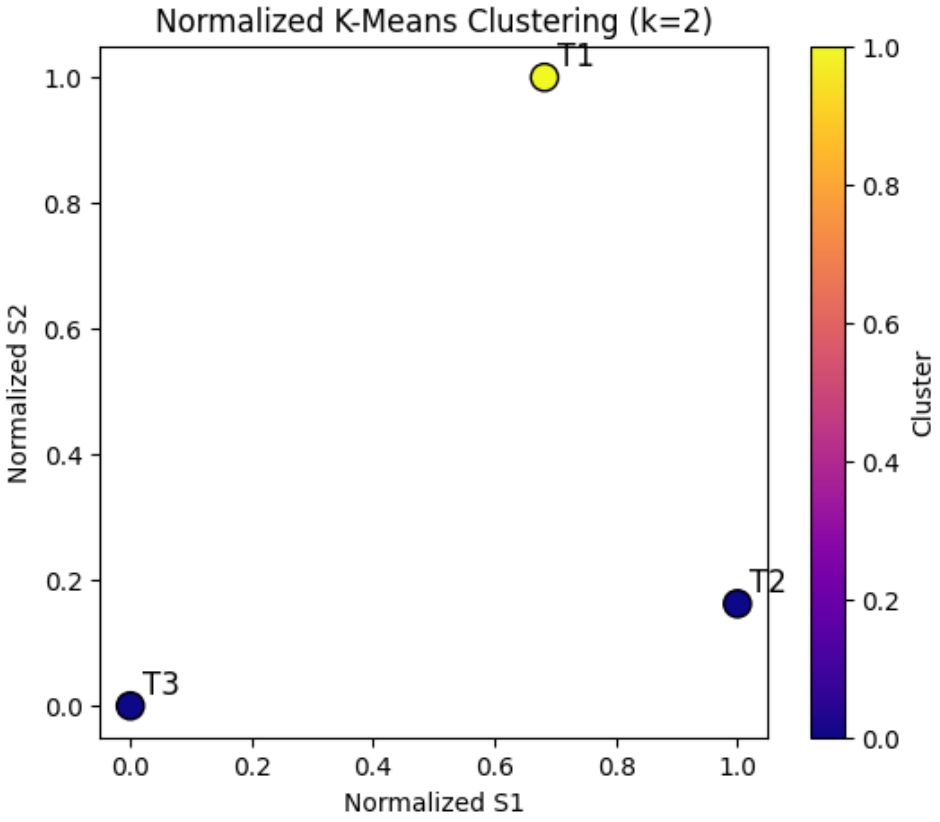

Figure 9

The Elbow Method (Fig. 10, left) and the Silhouette Method (Fig. 10, right) are used to determine the number of clusters (k) that produce the best result: the evaluation plots are clustering. Elbow Method: As k increases, inertia reduces. The inertia is at its highest (1.627) at $k = 1$, suggesting that the samples are packed together and that a satisfactory fit is not possible. The inertia value drops significantly (to 0.556) with $k = 2$, which improves the clustering efficiency significantly. By $k = 3$, inertia decreases to 0.000, but this is taking into account slight overfitting because each point is really a cluster of its own. The most mild compromise between simplicity and compactness is shown by the strong peak in k at 2. Plotting the silhouette score with $k = 2$ in the Silhouette Method yielded a result of 0.154. Despite its tiny size, this score is encouraging because it shows that clusters can be dispersed but are not very firmly linked together. Nonetheless, it favors the partition $k = 2$ as the data's most important partition. Overall, $k = 2$ is determined to be the optimal number of clusters by both evaluation tools. This is demonstrated by the Elbow Method's reduction of inertia and the Silhouette Method's maximum score, albeit at a moderate level.

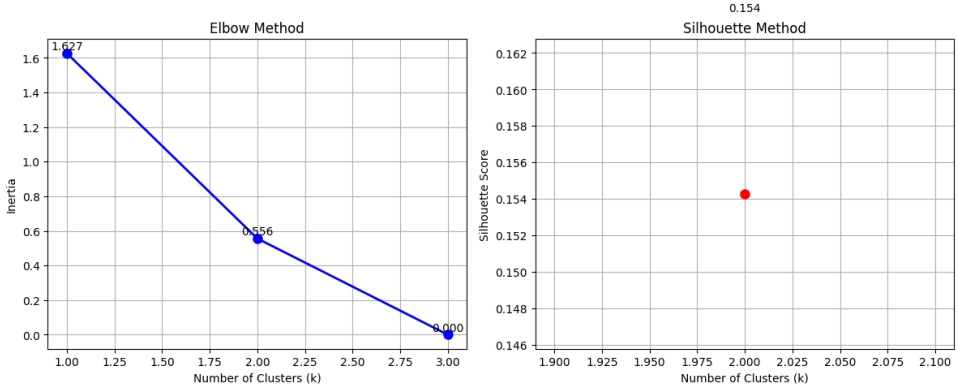

Figure 10

The Pearson correlation matrix of variables ($B_1 - B_4$ and Cot SM) is shown in a 3D surface plot in Fig. 11; the correlation value is shown in both surface height and color intensity. The degree of linear association is shown by the scale, which ranges from 0.76 (lower and dark purple) to 1.00 (higher and brilliant yellow/green). When it comes to Cot SM, the self-correlation between Cot SM and Cot SM should be at most 1.00, creating a tall peak at each axis junction. Cot SM has high relationships with these factors, as evidenced by the strong correlations found between it and B_1 (0.96) and B_3 (0.95). Cot SM (0.96) and the same (1.00) both display the highest values in the case of B_1. It shows moderate correspondence between dimensions, with lower but positive correlation coefficients with B_2 (0.77) and B_4 (0.81). Compared to other variables, B_2 exhibits a lower trend. Its values against Cot SM (0.76) and B_1 (0.77) are around the bottom spectrum, making it the weakly aligned variable, even though it still has a moderate correlation with B_3 (0.81) and B_4 (0.77). It is discovered that B_3 has a strong connection with both Cot SM (0.95) and B_3 (1.00). Although B 3 falls into the category of more potent influencers, other combinations, such as those with B_2 (0.81) and B_4 (0.77), are intermediate. B_4 has a strong association with Cot SM (0.85) and B_1 (0.81), and its correlation with itself is equal to 1. It has lower and more steady B_2 (0.77) and B_3 (0.77) values. The most dependable and resilient variables in the summary are Cot SM, B_1, and B_3, all of which have a constant correlation with one another (0.95). The values on the lower end of the scale (0.76 -0.81) indicate that B_2 is the weakest contributor, whereas B_4 is somewhat aligned.

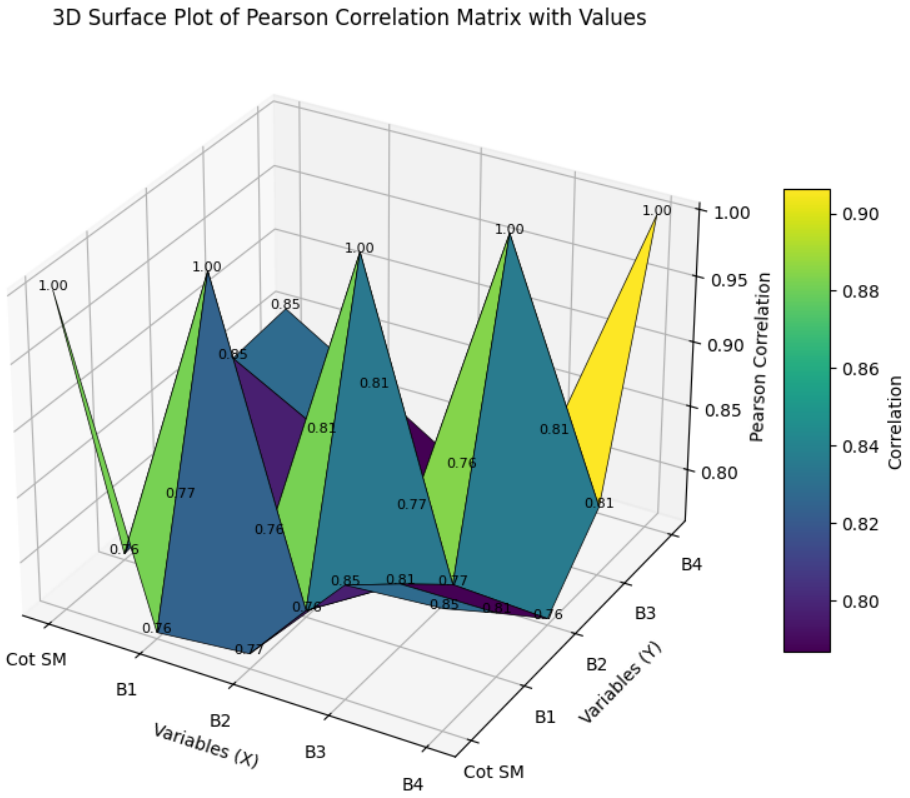

Figure 11

The normalized Pearson correlation matrix of the variables ($B_1 - B_4$ and Cot SM) is shown in Fig. 12 as a 3D surface plot with values scaled from 0.0 to 1.0. The surface's peaks and color shading (red for lower correlations, blue for higher correlations) show the relative values of associations after normalization. As expected, the diagonal self-correlation in the Cot SM instance is 1.00. Off-diagonal values typically show weak normalized connections, such as 0.00 with B_2 and 0.00 with B_4. Only a mild peak (0.35) is seen in Cot SM-B_1, suggesting a weak but comparatively stronger link. The diagonal (1.00) and Cot SM (0.35), in the instance of B 1, have the highest values. However, its impact on variables is weakly standardized, and its association with B_2 (0.03) and B_3 (0.19) is not significant. The values for B_2 are consistently around the bottom of the scale, with B_3 showing the strongest correlation. This yields B_2 the lowest normalized correlation, and B_3 the highest normalized correlation on its diagonal (1.00) and secondary values of 0.19 to B_1 and 0.17 to B_4, but virtually zero elsewhere. This suggests that B_3 is not dominant but rather moderately orientated. The diagonal maximum in B_4 is 1.00, and Cot SM has the strongest off-diagonal value (0.21). The others are weak (e.g., $B_2 = 0.02$, $B_3 = 0.17$), but B_4 falls in the middle of the normalized strength range. In summary, Cot SM and B_1 are highlighted as somewhat stronger factors by the normalized correlation surface; yet, their peaks are smaller than those of the un-normalized matrix. B_2 is always the weakest, followed by B_3 and B_4, which are average but dispersed. The overall pattern indicates that contrast has decreased after normalization, when the strongest correlations are highlighted.

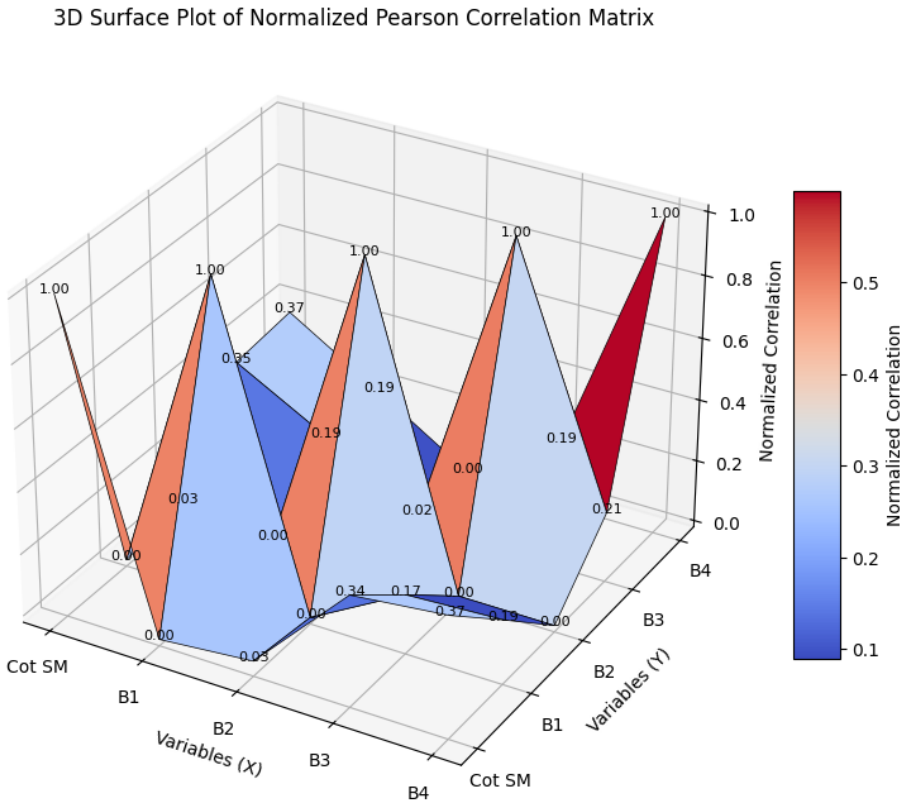

Figure 12

7. Aspect-Method Hybrid Analysis of Signal-Template

A multifaceted view of signal-template alignment is provided by combining aspect-based interpretation (based on stability, representativeness, and target divergence) with method-based evaluation (PCA, K-Means, t-SNE, spline smoothing, correlation analysis). Because it considers the possibility that the targets may be powerful in one analytical perspective and weak in another, such a hybrid structure does not rely too heavily on any one viewpoint. Since both theoretical and practical approaches can be used to support the ideas, the combination of the elements and approaches gives the outcomes their strength.

7.1. Aspect-based Analysis

Three main criteria can be used to view the targets ($T_1 - T_3$) from an aspectual perspective: stability, divergence, and representativeness. The most representative objective is usually T_1. Its proximity to Cluster C_2's centroid in 2D and 3D PCA projections further demonstrates that it is at the center of the data structure. K-Means and K-Means++ plots support this, showing that T_1 has the worldwide maximum similarity (0.665 at S_2) and is therefore utilized as a cluster formation indication. The extreme values of T_1 (0.0,1.0) in normalized clustering with (Fig. 9) further strengthen its hegemony. T_2 denotes average yet distinctive behavior. It regularly adopts intermediate positions and does not adhere to any centroid. It appears to be an outlier on PC 2 (i.e., in a high position, showing variability) in PCA (2D and 3D). Its partial divergence, which is not significant enough to be coherently destabilizing but significant enough to be dominating, is shown by K-Means plots, which position it with T_3 but align more with S_1. The least stable is always T_3. It wanders to the negative axes in PCA, which are not at the center but rather weakly connected to C_1. It belongs to the same group as T_2 in clustering, but its raw and normalized similarity scores are the lowest. Due to its location close to the

bottom-left quadrant or the divergent and weak alignment, it is either the most unreliable or the most steady target. Thus, aspect-wise hierarchy: $T_1 = Strongest(stable, representative) \rightarrow T_2 = Intermediate(divergent, transitional) \rightarrow T_3 = Weakest(unstable, marginal)$.

7.2. Method-based Analysis

The information presented by both methods shows that the target relationships are multi-faceted. Method-based comparison makes it easier to see how different approaches both complement and contradict one another rather than handling them independently. PCA does not result in variance loss and reduces dimensional complexity (PC1 = 0.65, PC2 = 0.35). It indicates that T_2 is central in C_2, that T_2 is an outlier, and that T_3 is marginal. The 3D image, which shows the intermediate position of T_2 and the negative position of T_3 along PC1/PC3, helps to narrow this down. PCA works well for structural mapping and visibility. The explicit grouping is the main focus of K-Means and K-Means++. The circled maximum (0.665) indicates that T_1 pulls its own odd cluster (Cluster 1, yellow). T_2 and T_3 are grouped together in weaker groups that show diminished commonality. K-Means++ refines the results by using centroid separation and maxima marking. Structural cohesiveness is justified by the extended clustering of Iris PCA enhancements, which show broader purple/yellow clusters and tight teal clusters. This pertains to the situation where representativeness (T_1 even teal) and divergence (T_2 T_3 purple/yellow) are explained by tight versus loose clusters. Relational overlaps are shown via t-SNE. T_2 cuts across groups and fully overlaps T_1 and T_3, much like versicolor in Iris. T_1 is comparable to setosa in that most of them are distinct, stable, and free of overlaps. Similar to virginica, T_3 is tiny but crosses boundaries. This method brings to light edge effects and transition regions that PCA misses. Spline-smoothed functional curves, which show a wave-like trend with local dips and a global maximum of 0.83, are indicative of functional variability. The idea that similarity is a dynamic process where T_1 predominates with peak alignment rather than a linear phenomenon is supported by this, which shows periodic changes that clustering cannot explain. Relationships between variables and targets are shown by Pearson correlation surfaces. While normalization reduces contrast, leaving only T_1B_1 reasonably robust, raw correlations (Cot SM of B_1 and B_3 are over 0.95), on the other hand, have significant stability markers. Because raw views overemphasize strength and normalized views downplay complexity, this dichotomy is harmful to presumptions. Method-wise convergence: All of the approaches concur that T_1 is superior and T_3 is inferior. The evaluation of T_2 is the only area where there is a difference: PCA classifies it as an outlier, K-Means pairs it with T_3, and t-SNE classifies it as transitional. The methodology of triangulation shows that T_2 is neither totally stable nor entirely marginal; rather, its identity is contingent upon the method employed.

8. Four- Dimensional Evaluation of Analytical Techniques

To ascertain the efficacy of each analytical technique, the similarity relationships between targets $T_1 - T_3$ are also assessed by combining aspect-based and method-based techniques. The four evaluation dimensions-visibility, associativity, dynamicity, and scalability-are used to standardize comparisons. To provide a quantitative basis, numerical results of PCA loadings, Cot SM maximum, clustering inertia, silhouette results, and correlation coefficients are included.

Table 4: Aspect-Method Hybrid Evaluation of Analytical Techniques

Factors	**PCA(2D/3D)**	**K-Means/K-Means++**	**t-SNE(3D, Parallel Coordinates)**	**Spline-Smoothed Curves**	**Correlation Surfaces(Raw/Normalized)**
Visibility	Strong(PC1=0.65, PC2=0.35;$T-1 \rightarrow C_2$, T_2 high PC2, T_3 bottom left)	Very Strong(Global max 0.665 at $T_1 - S_2$ circled; centroids shown by X)	Strong(distinct separation: Setosa-like=T_1, transitional overlap=T_2, marginal=T_3)	Strong(global max Y=0.83 at $X \approx 8$ clearly highlighted)	Very Strong raw(Cot SM-B_1=0.96, B_3=0.95); Weak normalized(Cot SM-B_1=0.35 only)
Associativity	Strong($T_1 \leftrightarrow C_2; T_3 \leftrightarrow C_1 weakly$)	Strong(T_2,T_3 in Cluster 0; T_1 independent cluster)	Strong(overlap patterns: T_2 bridges T_1&T_3)	Medium-Strong(peaks/troughs reflect secondary associations)	Strong raw(B_1&B_3 tightly linked to Cot SM,$\geq$ 0.95); Weak normalized(0.00-0.21 across others)
Dynamicity	Medium(stable projection, $PC3 \approx 0$ adds little variance)	Strong(Elbow: inertia drop 1.627 $\rightarrow$ 0.556 at k=2; Silhouette=0.154)	Strong(interlacing of trajectories shows transitional dynamics)	Very Strong(wave cycle: rise 0.26 $\rightarrow$ 0.73, dip -0.54, peak 0.83)	Medium(raw exaggerates highs; normalization suppresses contrast, exposing fluctuation sensitivity)
Scalability	Strong(2D/3D scale interpretable with few targets; PC loadings stable)	Medium-Strong(works for k=2 but trivializes at k=3 with inertia=0.000)	Medium (good for small samples; overlaps increase with more classes)	Strong(generalizable trend pattern)	Medium (Raw shows clear peaks; normalization reduces contrast to near 0-0.35, weaker scaling)

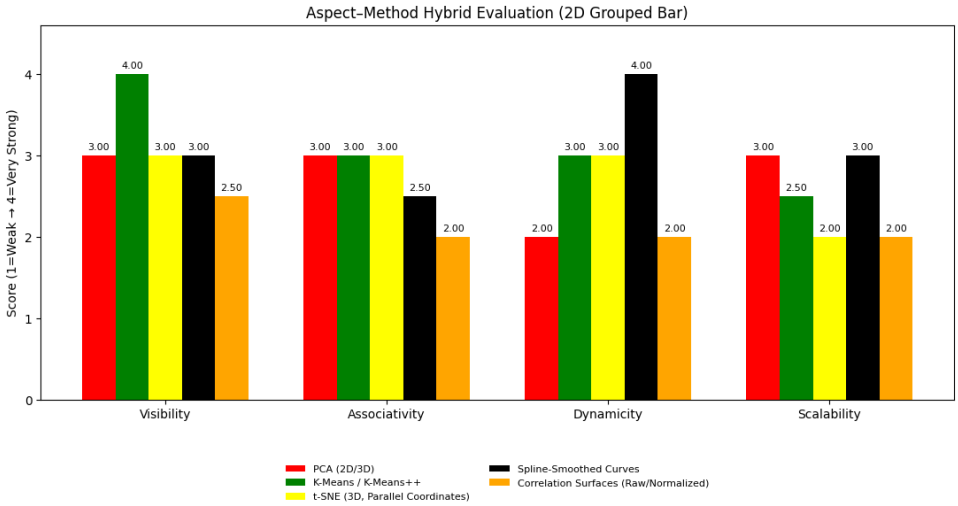

Figure 13

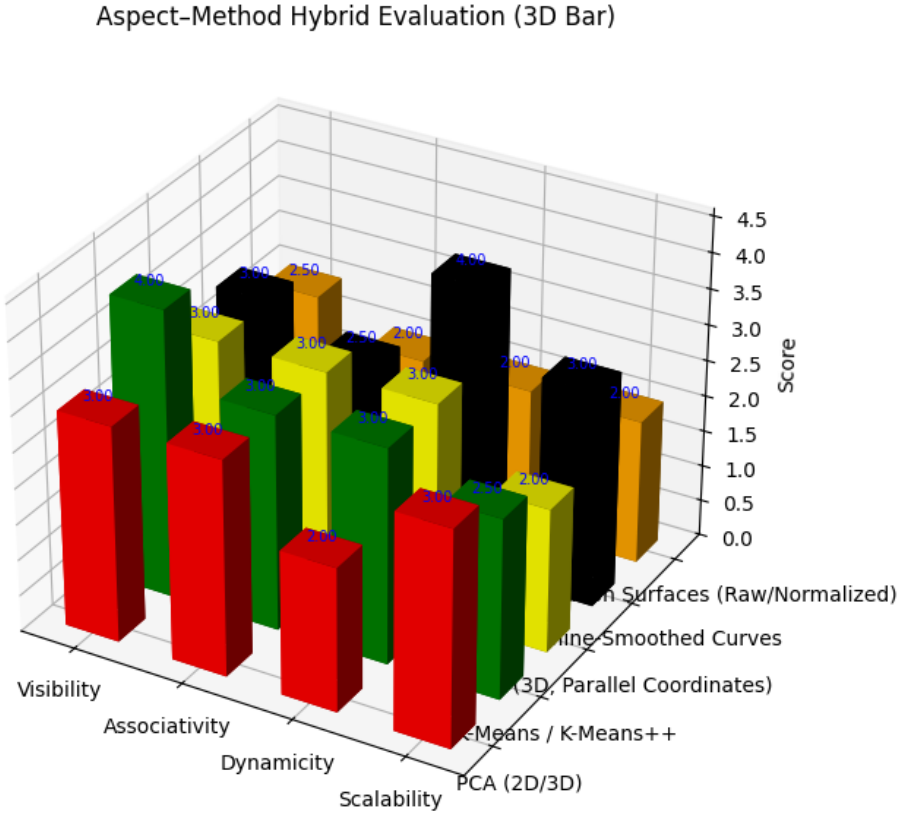

Figure 14

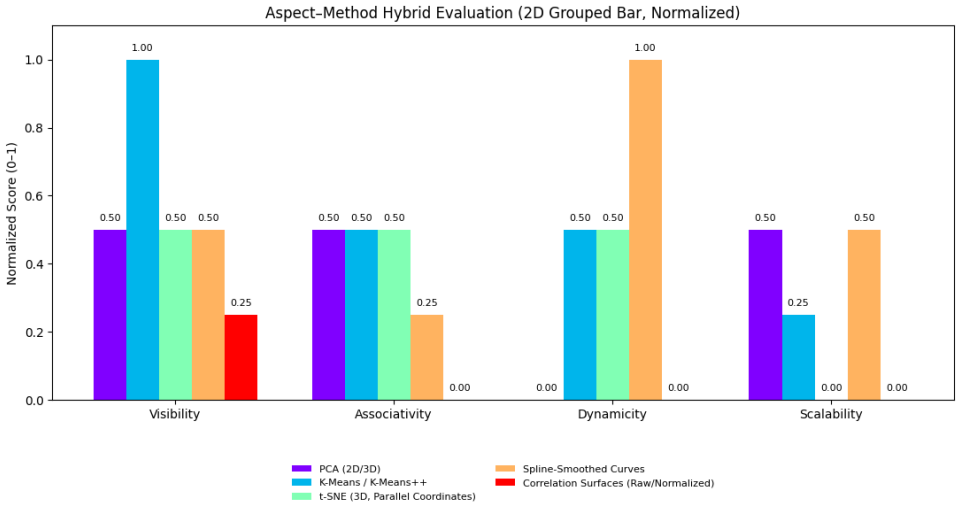

Figure 15

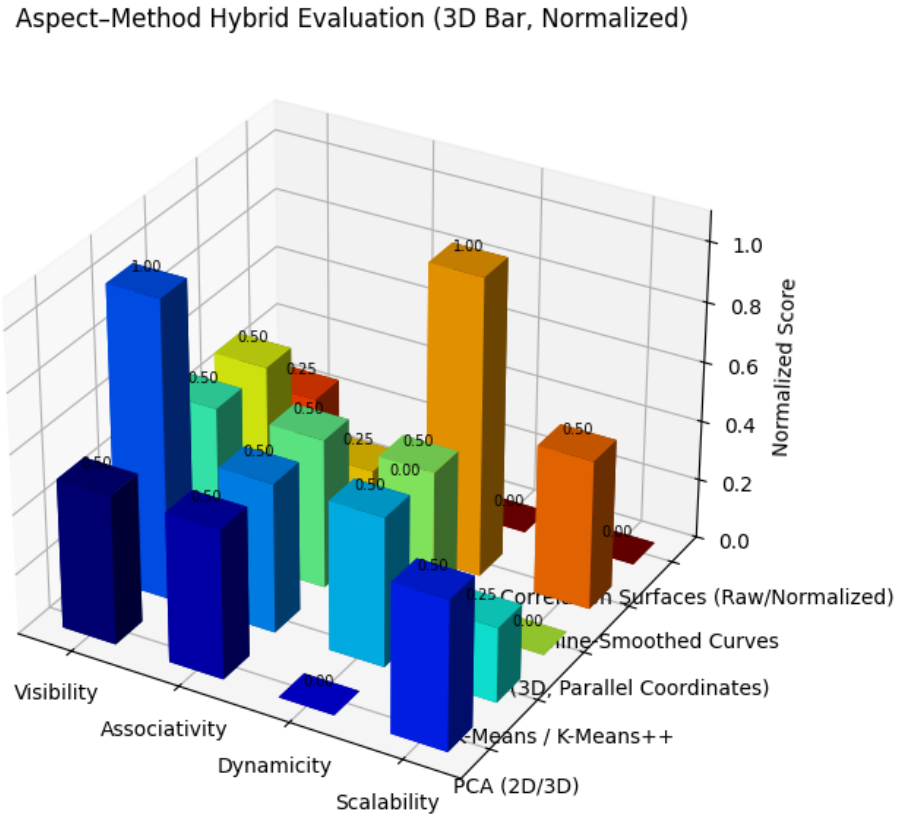

Figure 16

9. Conclusion

The targets show a consistent hierarchy, according to the relative comparison of PCA, K-Means, K-Means++, t-SNE, correlation surfaces, and spline-smoothed curves. T_1 consistently yields the worldwide maximum similarity values and is the strongest and most representative target. It also exactly fits the centroid. T_2 is transitional or unsteady because it acts as an intermediary, rotating between clustering with T_3 (K-Means) and being an outlier (PCA). T_3 will be the least coherent and weakest target; it will be situated on the border between methods

and be only loosely connected to Cluster C_1. T_1 is structurally dominating, T_2 is method dependent, and T_3 is marginal, according to this triangulation methodology. A powerful hybrid perspective on the interpretation of signal-template alignment is provided by combining aspect (representativeness, stability, and divergence) and method-based techniques.

10. Limitations

There are several limitations to the analysis. Because it only focuses on three targets (T_1−T_3) and the signals associated with them, the dataset itself is likewise narrow and low in scope, which restricts the potential to extrapolate the results to more complicated or broad datasets. The third principal component in PCA, PC3 = 0, adds very little variance, which lowers the 3D projections' informative value and could be deceptive about nonlinear relationships. Since T_2 behavior is susceptible to algorithmic assumptions rather than consistent structural identity, it is very method-dependent and alternates between outlier and transitional behavior when PCA, K-Means, or t-SNE are applied. The fact that the Elbow and Silhouette algorithms agree on k = 2, but the silhouette score (0.154) suggests a weak cohesiveness and separation, is another flaw in the algorithm that cluster validation highlights. Because scaling reduces the contrast of correlation matrices, normalization introduces an extra constraint that tends to overemphasize homogeneity and obscure important correlations. Finally, the framework cannot be used to real-time or changing data settings because it is static and requires constant similarity scores and projections without taking into account temporal or dynamic modification of signal behavior.

11. Future work

There are several ways that future study can fill in the gaps in this paradigm. Larger, higher-dimensional datasets with more targets and signals to be expanded can be used to demonstrate scalability and stability. To find structural nuances that linear PCA might miss, nonlinear dimensionality reduction techniques like kernel PCA or UMAP may be added. Temporal clustering or streaming PCA could be used to improve the way signals evolve over time and get around the framework's current static nature. It is possible to integrate fuzzy-based or neutrophilic multi-criteria decision-making techniques to effectively handle uncertainty, particularly when dealing with transitional goals like T_2. In order to make the hierarchy more structured and flexible, the hybrid aspect-method model can also be improved by adding the weighted evaluation of visibility, associativity, dynamicity, and scalability. Validation across a range of applications, such as financial data, biomedical signal processing, and military surveillance, would demonstrate robustness and transferability. Finally, to improve the framework's practicality on a real-time or even large-scale basis, automated visualization pipelines of PCA, K-Means, t-SNE, and spline smoothed curves should be added. This will eliminate manual bias and simplify understanding.

Acknowledgements

The authors extend their appreciation to the Deanship of Scientific Research at Northern Border University, Arar, KSA for funding this research work through the project number "NBU-FFR-2025-2727-11".

Conflicts of Interest: The authors declare that there are no conflicts of interest regarding the publication of this paper.

Availability of Data and Materials: All the data and materials are provided in the manuscript.

References

[1] Y. Al-Qudah, N. Hassan, Operations on complex multi-fuzzy sets. *Journal of Intelligent and Fuzzy Systems*, vol. 33(3), pp. 1527-1540, 2017.

[2] H. Garg, D. Rani, Complex interval-valued intuitionistic fuzzy sets and their aggregation operators. *Fundamenta Informaticae*, vol. 164(1), pp. 61-101, 2019.

[3] H. Garg, T. Mahmood, A. U. Rehman, Ali, Z. CHFS: Complex hesitant fuzzy setstheir applications to decision making with different and innovative distance measures. *CAAI Transactions on Intelligence Technology*, vol. 6(1), pp. 93-122, 2021.

[4] P. K. Singh, Complex vague set based concept lattice. *Chaos, Solitons and Fractals*, vol. 96, pp. 145-153, 2017.

[5] S. RaBroumi, A. Bakali, M. Talea, F. Smarandache, P. K. Singh, V. Uluay, M. Khan, Bipolar complex neutrosophic sets and its application in decision making problem. In *Fuzzy Multi-criteria Decision-Making Using Neutrosophic Sets*; Springer: Cham, pp. 677-710, 2019.

[6] S. G. Quek, S. Broumi, G. Selvachandran, A. Bakali, M. Talea, F. Smarandache, Some results on the graph theory for complex neutrosophic sets. *Symmetry*, vol. 10(6), art. 190, 2018.

[7] A. Al-Quran, S. Alkhazaleh, Relations between the complex neutrosophic sets with their applications in decision making. *Axioms*, vol. 7(3), art. 64, 2018.

[8] L. Q. Dat, N. T. Thong, M. Ali, F. Smarandache, M. Abdel-Basset, H. V. Long, Linguistic approaches to interval complex neutrosophic sets in decision making. *IEEE Access*, vol. 7, pp. 38902-38917, 2019.

[9] D. Molodtsov, Soft set theory-first results. *Comput. Math. Appl.* vol. 37, pp. 19-31, 1999.

[10] P.K. Maji, R. Biswas, A. R. Roy, Fuzzy soft sets. *J. Fuzzy Math.* vol. 9, pp. 589-602, 2001.

[11] P.K. Maji, R. Biswas, A.R. Roy, Intuitionistic fuzzy soft sets. *J. Fuzzy Math.* vol. 9(3), pp. 677-692, 2001.

[12] B. Chetia, P. K. Das, An application of interval-valued fuzzy soft. *Int. J. Contemp. Math. Sci.* vol. 5(38), pp. 1887-1894, 2010.

[13] Y. Jiang, Y. Tang, Q. Chen, H. Liu, J. Tang, Interval-valued intuitionistic fuzzy soft sets and their properties. *Comput. Math. Appl.* vol. 60(3), pp. 906-918, 2010.

[14] P.K. Maji, Neutrosophic soft set. *Ann. Fuzzy Math. Inform.* vol. 5, pp. 157-168, 2013.

[15] I. Deli and S. Broumi, Neutrosophic soft relations and some properties, *Annals of Fuzzy Mathematics and Informatics*, vol. 9(1), pp. 169-182, 2015.

[16] T.Bera and N. K. Mahapatra, Introduction to neutrosophic soft topological space, Opsearch, vol. 54(4), pp. 841-867, 2017.

[17] I. Deli, Interval-valued neutrosophic soft sets and its decision making. *Int. J. Mach. Learn. Cyber.* vol. 8(2), pp. 665-676, 2017.

[18] M. Abu Qamar, N. Hassan, An approach toward a Q-neutrosophic soft set and its application in decision making. *Symmetry*, vol. 11(2), art. 139, 2019.

[19] M. Abu Qamar, A.G. Ahmad, N. Hassan, On Q-neutrosophic soft fields. *Neutrosophic Sets Syst.* vol. 32, pp. 80-93, 2020.

[20] P. Thirunavukarasu, R. Suresh, V. Ashokkumar, Theory of complex fuzzy soft set and its applications. *Int. J. Innov. Res. Sci. Technol.* vol. 3(10), pp. 13-18, 2017.

[21] G. Selvachandran, P. K. Singh, Interval-valued complex fuzzy soft set and its application. *Int. J. Uncertain. Quantif.* vol. 8(2), 2018.

[22] T. Fujita. The Hyperfuzzy VIKOR and Hyperfuzzy DEMATEL Methods for Multi-Criteria Decision-Making. *Spectrum of Decision Making and Applications*, vol. 3(1), pp. 292-315, 2025.

[23] R. Gul. An Extension of VIKOR Approach for MCDM Using Bipolar Fuzzy Preference d-Covering Based Bipolar Fuzzy Rough Set Model. *Spectrum of Operational Research*, vol. 2(1), pp. 72-91, 2025.

[24] M. E. M. Abdalla, A. Uzair, A. Ishtiaq, M. Tahir., & M. Kamran. Algebraic Structures and Practical Implications of Interval-Valued Fermatean Neutrosophic Super Hyper Soft Sets in Healthcare. *Spectrum of Operational Research*, vol. 2(1), pp. 199-218.

[25] M. AlAkram, U. Amjad, J. C. R. Alcantud and G. Santos-Garcia, Complex Fermatean Fuzzy N-Soft Sets: A New Hybrid Model with Applications. *J. Ambient Intell. Humaniz. Comput.*, vol. 13, pp. 1-34, 2022.

[26] A. Al-Quran, S. Alkhazaleh, L. Abdullah, Complex Bipolar-Valued Neutrosophic Soft Set and its Decision Making Method. *Neutrosophic Sets Syst.* vol. 47, pp. 105-116, 2021.

[27] M. Akram, M. Shabir, A. Ashraf, Complex neutrosophic N-soft sets: A new model with applications. *Neutrosophic Sets Syst.* vol. 42, pp. 278-301, 2021.

[28] A. Al-Quran, N. Hassan, The complex neutrosophic soft expert relation and its multiple attribute decision-making method. *Entropy*, vol. 20, art. 101, 2018.

[29] F. Al-Sharqi, A. Al-Quran, A. G. Ahmad, S. Broumi, Interval-valued complex neutrosophic soft set and its applications in decision-making. *Neutrosophic Sets Syst.* vol. 40, pp. 149-168, 2021.

[30] F. Al-Sharqi, A. Al-Quran, A. G. Ahmad, Interval-Valued Neutrosophic Soft Expert Set from Real Space to Complex Space. *Comput. Model. Eng. Sci.* vol. 132(1), pp. 267-293, 2022.

[31] F. Al-Sharqi, A. Al-Quran, A. G. Ahmad, Interval complex neutrosophic soft relations and their application in decision-making. *J. Intell. Fuzzy Syst.* vol. 43(1), pp. 745-771, 2022.

[32] M. Saqlain, N. Jafar, S. Moin, M. Saeed, S. Broumi, Single and multi-valued neutrosophic hypersoft set and tangent similarity measure of single valued neutrosophic hypersoft sets. *Neutrosophic Sets Syst.* vol. 32(1), pp. 317-329, 2022.

[33] S. Begam S, G. Selvachandran, T. T. Ngan, R. Sharma, Similarity measure of lattice ordered multi-fuzzy soft sets based on set theoretic approach and its application in decision making. *Mathematics*, vol. 8(8), art. 1255, 2020.

[34] R. M. Zulqarnain, I. Siddique, M. Asif, S. Ahmad, S. Broumi, S. Ayaz, Similarity Measure for m-Polar Interval Valued Neutrosophic Soft Set with Application for Medical Diagnoses. *Neutrosophic Sets Syst.* vol. 47(1), pp. 147-164, 2021.

[35] D. Liu, G. Liu, Z. Liu, Some similarity measures of neutrosophic sets based on the Euclidean distance and their application in medical diagnosis. *Comput. Math. Methods Med.*, art. 9, 2018.

[36] K. Ullah, T. Mahmood, N. Jan, Similarity measures for T-spherical fuzzy sets with applications in pattern recognition. *Symmetry*, vol. 10(6), art. 193, 2018.

[37] A. U. Rahman, M. Saeed, H. A. E. W. Khalifa, W. A. Afifi, Decision making algorithmic techniques based on aggregation operations and similarity measures of possibility intuitionistic fuzzy hypersoft sets. *AIMS Math.* vol. 7(3), pp. 3866-3895, 2021.

[38] S. Broumi, F. Smarandache, Several Similarity Measures of Neutrosophic Sets. *Neutrosophic Sets Syst.* vol. 1, pp. 54-62, 2013.

[39] J. Ye, Similarity measures between interval neutrosophic sets and their applications in multi criteria decision-making. *J. Intell. Fuzzy Syst.* vol. 26(1), pp. 165-172, 2014.

[40] A. Mukherjee, S. Sarkar, Several similarity measures of interval valued neutrosophic soft sets and their application in pattern recognition problems. *Neutrosophic Sets Syst.* vol. 6, pp. 55-61, 2014.

[41] M. Abu Qamar, N. Hassan, Entropy, measures of distance and similarity of Q-neutrosophic soft sets and some applications. *Entropy*, vol. 20(9), art. 672, 2018.

[42] Y. Al-Qudah, N. Hassan, Complex multi-fuzzy soft set: Its entropy and similarity measure. *IEEE Access*, vol. 6, pp. 65002-65017, 2018.

[43] G. Selvachandran, H. Garg, M. H. Alaroud, A. R. Salleh, Similarity measure of complex vague soft sets and its application to pattern recognition. *Int. J. Fuzzy Syst.*, vol. 20(6), pp. 1901-1914, 2018.

[44] D. Xu, X. Cui, L. Peng, H. Xian, Distance measures between interval complex neutrosophic sets and their applications in multi-criteria group decision making. *AIMS Math.* vol. 5(6), pp. 5700-5715, 2020.
[45] F. Smarandache, Neutrosophic set, a generalisation of the intuitionistic fuzzy sets. *Int. J. Pure Appl. Math.* vol. 24, pp. 287-297, 2005.
[46] L. A. Zadeh, Fuzzy sets, *Information and Control*, vol. 8, pp. 338-353, 1965.
[47] F. Smarandache, Neutrosophy: Neutrosophic Probability, Set and Logic; *American Research Press: Rehoboth, IL, USA*, 1998.
[48] H. Wang, P. Madiraju, Y. Zhang, R. Sunderraman, Interval Neutrosophic Sets. *arXiv* 2004, math/0409113.
[49] A. Khalid, M. Abbas, Distance measures and operations in intuitionistic and interval-valued intuitionistic fuzzy soft set theory. *Int. J. Fuzzy Syst.*, vol. 17(3), pp. 490-497, 2015.
[50] F. Smarandache, Extension of Soft Set to HyperSoft Set, and then to Plithogenic Hypersoft Set. *Neutrosophic Sets Syst.* vol. 22, pp. 168-170, 2018.
[51] M. M. Abed, N. Hassan, F. Al-Sharqi, On Neutrosophic Multiplication Module. *Neutrosophic Sets Syst.* vol. 47, pp. 198-208, 2022.
[52] N. A. Alhaleem, A.G. Ahmad,Intuitionistic Anti Fuzzy Normal Subrings over Normed Rings. *Sains Malays.* vol. 51(2), pp. 609-618, 2022.
[53] F. G. Al-Sharqi, M. M. Abed, A. A. Mhassin, On Polish Groups and their Applications. *J. Eng. Appl. Sci.* vol. 13(18), pp. 7533-7536, 2018.
[54] M. M. Abed, F. Al-Sharqi, S. H. Zail, A Certain Conditions on Some Rings Give P.P. Ring. *J. Phys. Conf. Ser.* vol. 1818, art. 012068, 2021.
[55] M. M. Abed, F. G. Al-Sharqi, Classical Artinian module and related topics. *J. Phys. Conf. Ser.* vol. 1003, art. 012065, 2018.
[56] M. M. Abed, F. G. Al-Sharqi, A. A. Mhassin, Study fractional ideals over some domains. *AIP Conf. Proc.* vol. 2138, art. 030001, 2019.
[57] M. M. Abed, A. F. Al-Jumaili, F. G. Al-sharqi, Some mathematical structures in a topological group. J. *Algebra Appl. Math.* vol. 16(2), pp. 99-117, 2018.
[58] M. M. Abed, F. G. Al-Sharqi, Classical Artinian module and related topics. *J. Phys. Conf. Ser.* vol. 1003, art. 012065, 2018.
[59] A. F. Al-Jumaili, M.M. Abed, F. Al-Sharqi, Other new types of Mappings with Strongly Closed Graphs in Topological spaces via $e-\theta$ and $\delta-\beta-\theta$ open sets. *J. Phys. Conf. Ser.*, vol. 1234, art. 012101, 2019.
[60] S. A. El-Sheikh, & A. M. Abd El-Latif. Decompositions of some types of supra soft sets and soft continuity. *Int. J. Math. Trends Technol.*, vol. 9(1), pp. 37-56, 2014.
[61] A. M. Abd El-Latif, & R. A. Hosny. Supra open soft sets and associated soft separation axioms. *Int. J. Adv. Math.*, vol. 6, pp. 68-81, 2017.
[62] A. M. Abd El-Latif. Soft supra strongly generalized closed sets. *J. Intell. Fuzzy Systems*, vol. 31(3), pp. 1311-1317, 2016.
[63] A. M. Abd El-Latif, & R. A. Hosny. Soft supra extra strongly generalized closed sets. *An. Univ. Oradea Fasc. Mat.*, vol. 24(1), pp. 103-112, 2017.
[64] A. M. Abd El-Latif, & R. A. Hosny. Supra soft separation axioms and supra irresoluteness based on supra b-soft sets. *Gazi Univ. J. Sci.*, vol. 29(4), pp. 845-854, 2016.
[65] A. M. Abd El-Latif. Soft supra strongly *semi*$*$ generalized closed sets. *Ann. Fuzzy Math. Inform.*, vol. 13(1), pp. 63-71, 2017.
[66] A. M. Abd El-Latif, & R. A. Hosny. Supra semi open soft sets and associated soft separation axioms. *Appl. Math. Inf. Sci.*, vol. 10(6), pp. 2207-2215, 2016.
[67] A. M. Abd El-Latif. Supra soft *b*-connectedness II: Some types of supra soft *b*-connectedness. *Creat. Math. Inform.*, vol. 26(1), pp. 1-8, 2017.
[68] A. M. Abd El-Latif, & S. Karatas. Soft supra strongly generalized closed sets via soft ideals. *Appl. Math. Inf. Sci. Lett.*, vol. 5(1), pp. 21-26, 2016.

[69] A. M. Abd El-Latif. On soft supra compactness in supra soft topological spaces. *Tbil. Math. J.*, vol. 11(1), pp. 169-178, 2018.

[70] A. A. Abubaker, R. Hatamleh, K. Matarneh, & A. Al-Husban, On the Numerical Solutions for Some Neutrosophic Singular Boundary Value Problems by Using (LPM) Polynomials. *Int. J. of Neutro. Sci.*, vol. 25(2), pp. 197-205, 2024.

[71] A. Ahmad, R. Hatamleh, K. Matarneh, & A. Al-Husban, On the Irreversible k-Threshold Conversion Number for Some Graph Products and Neutrosophic Graphs. *Int. J. of Neutro. Sci.*, vol. 25(2), pp. 183-196, 2025.

[72] A. Rajalakshmi, R. Hatamleh, A. Al-Husban, K. L. Muthu Kumaran, & M. S. Malchijah raj, Various (ζ_1, ζ_2) neutrosophic ideals of an ordered ternary semigroups. *Comm. on Appl. Non. Ana.*, vol. 32(3), pp. 400-417, 2025.

[73] R. Hatamleh, A. Al-Husban, Sundareswari, G. K. Balaj, & M. Palanikumar, Complex Tangent Trigonometric Approach Applied to (γ, τ)-Rung Fuzzy Set using Weighted Averaging, Geometric Operators and its Extension. *Comm. on Appl. Non. Ana.*, vol. 32(5), pp. 133-144, 2025.

[74] R. Hatamleh, A. Al-Husban, N. Sundarakannan, & M. S. Malchijah Raj, Complex cubic intuitionistic fuzzy set applied to subbisemirings of bisemirings using homomorphism. *Comm. on Appl. Non. Ana.*, vol. 32(3), pp. 418-435, 2025.

[75] R. Hatamleh, & A. Hazaymeh, On Some Topological Spaces Based On Symbolic n Plithogenic Intervals. *Int. J. of Neutro. Sci.*, vol. 25(1), pp. 23-37, 2025.

[76] R. Hatamleh, & A. Hazaymeh, Finding Minimal Units In Several Two-Fold Fuzzy Finite Neutrosophic Rings. *Neutro. Set. and Syst.*, vol. 70, pp. 1-16, 2024.